Book of Abstracts

ESS-HPT 2015

The European Summer School in High Pressure Technology

Thomas Gamse (editor)

Impressum

Organisation: Thomas Gamse
Institute of Chemical Engineering and Environmental Technology
Central Lab Biobased Products
Graz University of Technology, Inffeldgasse 25/C, A-8010 Graz, Austria
Tel. +43 (0)316 873-7477
Email: Thomas.Gamse@TUGraz.at

Zeljko Knez
Amra Perva-Uzunalić
Faculty of Chemistry and Chemical Engineering
Laboratory for Separation Processes
University of Maribor, Smetanova ulica 17, 2000 Maribor, Slovenia
Email: zeljko.knez@um.si; amra.uzunalic@um.si

Editor: Thomas Gamse
Layout: Thomas Gamse
Cover: Thomas Gamse

ISBN (e-book) 978-3-85125-416-7
DOI 10.3217/978-3-85125-416-7

Preface

The European Summer School in High Pressure Technology (ESS-HPT) is the continuation of many years of high pressure intensive course. The history of this very successful series of courses started in 1995, when the first intensive course took place in Monselice, Italy. Most of these Intensive Courses were supported by SOCRATES and later Life Long Learning, as shown in following overview:

SOCRATES IP "Current Trends in High Pressure Technology and Chemical Engineering
- 1995 Monselice / Italy
- 1996 Nancy / France
- 1997 Erlangen / Germany

SOCRATES IP "High Pressure Technology in Process and Chemical Engineering"
- 1999 Abano Terme / Italy
- 2000 Valladolid / Spain
- 2001 Maribor / Slovenia and Graz / Austria

SOCRATES IP "High Pressure Chemical Engineering Processes: Basics and Applications"
- 2002 Graz / Austria and Maribor / Slovenia
- 2003 Budapest / Hungary
- 2004 Barcelona / Spain

SOCRATES IP "Basics, Developments, Research and Industrial Applications in High Pressure Chemical Engineering Processes
- 2005 Prague / Czech Republic
- 2006 Lisbon / Portugal
- 2007 Albi / France

Life Long Learning IP "SCF- GSCE: Supercritical Fluids – Green Solvents in Chemical Engineering
- 2008 Thessaloniki / Greece
- 2009 Istanbul / Turkey
- 2010 Budapest / Hungary

EFCE Intensive Course "High Pressure Technology - From Basics to Industrial Applications"
- 2011 Belgrade / Serbia

Life Long Learning IP "PIHPT: Process Intensification by High Pressure Technologies – Actual Strategies for Energy and Resources Conservation
- 2012 Maribor / Slovenia and Graz / Austria
- 2013 Darmstadt / Germany
- 2014 Glasgow / Great Britain

Unfortunately these Intensive Programmes were cancelled within ERASMUS+. The EFCE Working Party "High Pressure Technology" decided in September 2014 to go on with this course in the form of a Summer School.

The ESS-HPT will take place every year within the first 2 weeks of July at University of Maribor, Slovenia and Graz University of Technology, Austria.

All participants have to give an oral presentation and the abstracts of these presentations, which are peer-reviewed by the EFCE WP Members, are published in this book of abstract.

The editor

Thomas Gamse
Organiser of ESS-HPT 2015

Many thanks to our sponsors, NATEX Prozesstechnologie GesmbH and BASF SE Polymer Process Development.

Contents

Abstracts of Participants Presentations

Preparation of the shell material for the PGSS process application

Neven Tutnjevic, University of Maribor, Faculty of chemistry and chemical engineering;
Laboratory of separation processes and production design;
Smetanova 17, 2000 Maribor; neven.tutnjevic@um.si

With the high pressure technology PGSS (Particle from Gas Saturated Solutions) powders, which are difficult to achieve by classical methods like milling, spray drying or crystallization, can be produced. In the last years, PGSS process was used to produce micronized single components and in order to encapsulate different active compounds. In the PGSS process the substance or the mixture of substances to be powderised must be converted into a sprayable form by liquefaction/dissolution. This can be achieved by melting or/and dissolving the substance or mixture of substances in a liquid solvent, or by dispersing solids or liquids in a melt or solution, and saturation of the melt/solution/dispersion with the gas. PGSS process consists of melting the substance to be sprayed, mixing with super critical CO_2 and expansion into the spray tower where solid particles are obtained. Due to the reduced solubility after expansion the increased volume of the disappearing gas causes that liquid transforms into droplets. Due to the Joule-Thomson effect the gas cools down and the droplets solidify. Fine particles can be achieved and they are collected on the bottom of the spray tower. Besides powders also composites can be produced.

For the production of composites the shell and core materials are melted and pumped through the static mixer, where supercritical CO_2 is introduced. Afterwards the mixture is expanded through a nozzle into a spray tower operating at ambient pressure. Due to the Joule-Thomson effect of CO_2 solid particles are obtained almost immediately. Powders with a high loading of dispersed phase can be achieved.

Aim of this investigation was to obtain combinations of sugars, which could be used as shell material during the PGSS process for the encapsulation of different flavours. The physical properties of the shell material such as thermal stability and viscosity were investigated.

For the preliminary tests PEG 6000 was used as a model substance. Carbohydrates such as maltodextrin, D-sorbitol, dextrose, fructose, palatinose, sucrose, fructose syrup, sorbitol, corn syrup, fructose-glucose syrup, oligofructose syrup were used in order to determine suitable shell material.

Melting points of carbohydrates were measured using thermogravimetric (TG) method. It was observed that melting points of the carbohydrates were in the temperature range 95 – 240 °C.

120 different combinations of wall materials were analysed. Viscosity of the prepared carbohydrate mixtures was measured with the rotational rheometer. It was found out that only 24 samples were suitable for further processing due to the suitable viscosity in the temperature range 110-130 °C.

Investigating interfacial phenomena around critical point with capillary rise method

Gregor Kravanja

University of Maribor, Faculty of Chemistry and Chemical Engineering, Smetanova 17, SI-2000 Maribor, Slovenia, fax: +386 2 2516750, e-mail: gregor.kravanja@um.si

Investigations of basic thermodynamical and transport data like phase equilibria, density, viscosity, dielectric constant, diffusion coefficient and interfacial tension are fundamental for process design. Even if mathematical models can be used to predict the data at different conditions, these parameters should be first determined experimentally to find the suitable model and to confirm the fitting of the results to the model.

Since the interfacial tension plays a crucial role in the determination of interactions, interface stability and flow properties of reservoir fluids in the upstream and downstream processes of the petroleum industry and beside, deep natural gas resources are characterized by both abnormally high pore pressure and temperature gradients, there is a challenging task for engineers to investigate the interfacial interactions in the binary systems at extreme pressure and temperature conditions. There is a growing interest in storage of carbon dioxide in subsurface geologic formations, principally saline aquifers. There is a lack of data meeting the criteria for ensuring an accurate stability and long-term viability of geologic carbon storage despite the fact that injected CO_2 must be kept in place by an overlying cap rock of very low permeability. Consequently, interfacial tension measurements should couple the conditions pertinent to geologic carbon storage over the entire range of pressures and temperatures from 5.0 up to 45.0 MPa and 298 to 383 K. In addition, interfacial tension plays a key role in understanding many polymer processes such as

foaming, blending, coating and particle formation where low interfacial tension is desired due to the increase of the nucleation rate and production of small and uniform cells. Supercritical fluids are promising media for reducing interfacial tension and increasing solubility of gas into polymers melts.

Therefore, an optimized experimental setup to determine the interfacial tension and visualize the interfacial interactions phenomenon based on the capillary rise phenomena was developed that reflects a compromise between the competing claims of accuracy, low cost operation and simplicity 0. The new technique makes it possible to determine the interfacial tension and visualize the interfacial interactions phenomenon in the two component system of polymer and compressed CO_2. Capillary rise method was validated by conducting the measurements of the interfacial tension between CO_2 and pure water at a temperature of 298.25 K in pressure range from 0.1 MPa to 20.00 MPa. . Time, required to reach equilibria was determined experimentally and took approximately 5 min. To perform a measurement of interfacial tension at the CO_2+ water interface, a glassy capillary tube with a radius of 1.5 × 10−4m was placed inside the measuring cell. The radius of capillaries were determined by a laser coordinate measuring Machine Zeiss UMC Zeiss UMC. Since the meniscus can be difficult to see, a special camera was used to read the height of the liquid (*h*) in capillary and to observe the behavior of the system during the experiment in order to obtain reproducible results.

Interfacial tension at the CO_2 + PEG interface for the systems containing PEGs of different molecular weight (200, 400, 600) was measured in pressure range from 0.1 MPa up to 30.0 MPa at two different temperatures of 313 K and 333 K using Capillary Rise method, adapted to the measurement conditions and sample properties. The capillary rise method requires

previous knowledge about the density of the investigated systems. Density of CO_2 saturated solutions of polyethylene glycols (PEGs) was measured by a volumetric method, validated by determining density of pure CO_2 at different pressures and a temperature of 293 K or by gravimetric method involving magnetic suspension balance (MBS).

Investigated interfacial tension at the CO_2 + polyethylene glycol (PEG) interface for PEGs of different molar masses decreases with increasing pressure for all of the studied systems. The impact of temperature is small and the influence of molecular weight is almost negligible. Pressure is certainly found to play an important role when considering the interfacial behavior of the investigated systems. In case of thermo labile substances which may degrade at higher temperature that is certainly a preferred option of adjusting material properties.

Reference:

[1] Maša Knez Hrnčič, Gregor Kravanja, Mojca Škerget, Makfire Sadiku, Željko Knez, Investigation of interfacial tension of the binary system polyethylene glycol/CO2 by a capillary rise method, The Journal of Supercritical Fluids, Volume 102, July 2015, Pages 9-16, ISSN 0896-8446

Preparation of nanostructured TiO_2 and lanthanides doped TiO_2 from titanyl sulphate and by using pressurized water processing

Jaroslav Lang[1,2], Lukáš Polách[2] and Lenka Matějová[2]

[1]*Nanotechnology Centre, VŠB – Technical University of Ostrava, 17. listopadu 15/2172, 708 33 Ostrava-Poruba, Czech Republic*

[2]*Institute of Environmental Technology, VŠB – Technical University of Ostrava, 17. listopadu 15/2172, 708 33 Ostrava-Poruba, Czech Republic*

Presenting author email: jaroslav.lang@vsb.cz

Introduction

Titanium dioxide (TiO_2) is a common compound widely used in industry from food processing to pigment production [1]. TiO_2 is a semiconductor. In semiconductors photoinduced transition of electron from valence band to conductive band can occur. Photons with sufficient energy, higher than the energy of the band gap, are able to photoexcite electrons. The ability of semiconductor to transfer photoinduced electron to an adsorbed compound is determined by the band energy position and the redox potential of adsorbed compounds, and it is necessary for the progress of photocatalytic reactions. The photocatalytic reactions can be used for decomposition of pollutants, antimicrobial protection and self-cleaning surfaces. In titanium dioxide the band gap energy corresponds to photons in the UV region of light spectrum. The light can be supplied by a lamp or daylight. Via doping, charge carriers recombination can be decreased and TiO_2 surface properties can be altered, resulting in enhanced (photo)catalytic activity.

The most notable elements for TiO_2 doping are transition metals and lanthanides [2, 3]. The reason for doping is introduction of sub band states into the TiO_2 band gap and thus the decrease of the photoexcitation energy needed. Lanthanides affect the photocatalytic activity in several different ways: Their *4f* orbitals prevent recombination of photogenerated electron-hole pairs, can create complexes with Levis bases securing the reactant on the surface of TiO_2 [3]. Moreover, CeO_2-TiO_2 as well as Ce/TiO_2 show mesoporous structure with larger surface area than TiO_2 [4], improved structural stability [4] and anatase-to-rutile transformation temperature is shifted to higher temperatures [5].

Synthesis method itself greatly affects the microstructure of TiO_2 product. It determines whether it is amorphous or crystalline, what is the phase composition, crystallite size, crystal

lattice defects, surface properties, presence of impurities etc. The most common synthesis methods of TiO_2, sol-gel methods, use titanium alkoxides (e.g. titanium tetraisopropoxide, titanium tetrabutoxide or titanium tetra-tert-butoxide) as Ti sources, although other feasible methods and cheaper titanium precursors can be utilized. A hydrothermal method utilizing titanyl sulphate precursor belongs among less popular but widely used synthesis method in industry.

Titanyl sulphate ($TiOSO_4.H_2O$) is cheap, available and widely used raw material in pigment industry. $TiOSO_4.H_2O$ used in our experiments was supplied by Precheza a.s. (Czech Republic). Hydrothermal method uses calcination of the semi-product as a means to improve crystallinity and promote TiO_2 anatase phase crystallization. Pressurized hot (subcritical) water processing represents viable alternative to calcination, enabling better control over titania (micro)structural properties such as phase composition, crystallite size or crystal lattice defects. In fact, the (micro)structural properties affects crucially a final (photo)catalytic activity of semiconductor materials.

Objectives of the work

The goal of this work is preparation of nanostructured TiO_2 and lanthanides (Ce, Nd) doped TiO_2 from titanyl sulphate and by using pressurized hot water processing at different experimental conditions (temperature and pressure), characterization of (micro)structural, textural and optical properties and investigation of photocatalytic activity. The photocatalytic activity of synthesized materials is evaluated in the photo-oxidation of model azo-dye Acid Orange 7 and in the photocatalytic decomposition of N_2O. The relationship between the material microstructure and the photocatalytic activity in individual reactions should be revealed.

TiO_2 was prepared from colloid solution of titanyl sulphate by two methods: hydrothermal and nuclei method. TiO_2 was further processed with pressurized hot water at different temperatures (25-200°C) and pressures (10-30 MPa). The effect of different particle-size of precursor, temperature and pressure of subcritical water on TiO_2 crystallization was studied. TiO_2 structural properties were characterized by Raman spectroscopy and X-ray powder diffraction, textural properties such as the specific surface area and the pore volume were determined by nitrogen physisorption. UV-vis spectrometry and gas chromatography were used for evaluation of photocatalytic activity tests.

Experimental set-up for pressurized hot water processing

The pressurized hot water processing was carried out in a laboratory-made set-up equipped with a HPLC BETA10 Plus gradient pump (Ecom s.r.o., Czech Republic), a chromatographic oven operating in the temperature range of 25–400 °C, capillary cooling and a restrictor operating at ambient temperature. A scheme of the experimental set-up is shown in Fig. 1.

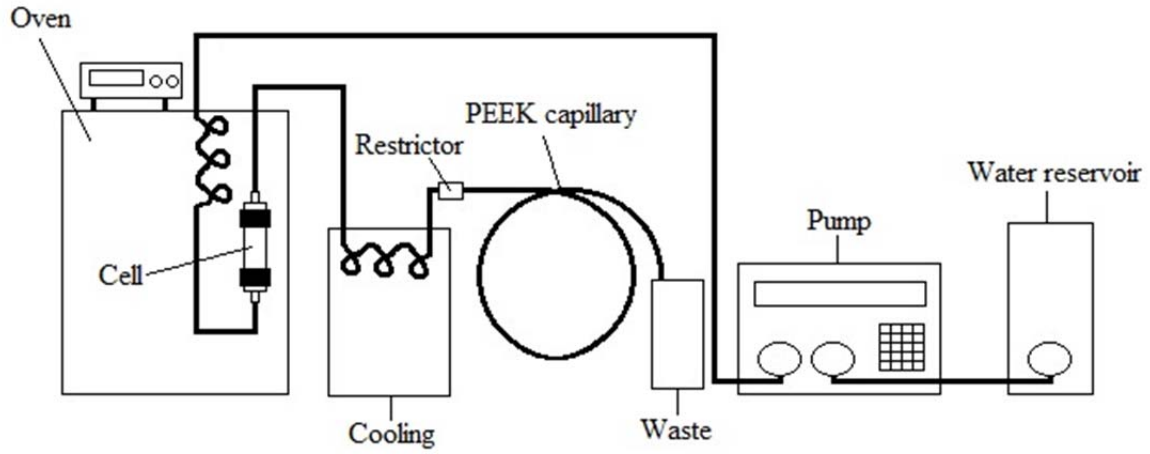

Fig.1. A scheme of set-up for pressurized hot water processing.

Current results

It was revealed that different particle-size of precursor treated by pressurized hot water processing does not affect TiO_2 crystal structure and crystallite-size. Contrary to pressure, the temperature of pressurized hot water plays the key role in TiO_2 crystallization. TiO_2 anatase from hydrothermally-prepared precursor shows significantly higher specific surface area and photocatalytic activity than TiO_2 anatase from nuclei-prepared precursor.

Acknowledgements

The financial support of the Grant Agency of the Czech Republic (project reg. No. 14-23274S) and the Ministry of Education, Youth, and Sports of the Czech Republic in the ‘‘National Feasibility Program I’’ (project reg. No. LO1208, ‘‘TEWEP’’) is gratefully acknowledged. Special thanks are devoted to Ing. Pavel Kovář and Precheza a.s. company.

References

[1] HALLAGAN, J.B., ALLEN, D.D., BORZELLECA, J.F.: The Safety and regulatory status of food, drug and cosmetic colour additives exempt from certification. *Food and Chemical Toxicology* 33(6) (1995) 515–591.

[2] ŠTENGL, V., BAKARDJIEVA, S., MURAFA, N.: Preparation and photocatalytic activity of rare earth doped TiO_2 nanoparticles. *Materials Chemistry and Physics* 114 (2009) 217–226.

[3] ZAINULLINA, V.M., ZHUKOV, V.P., KOROTIN, M.A.: Influence of oxygen nonstoichiometry and doping with 2p-, 3p-, 6p- and 3d-elements on electronic structure, optical properties and photocatalytic activity of rutile and anatase: Ab initio approaches. *Journal of Photochemistry and Photobiology C: Photochemistry Reviews* 22 (2015) 58–83.

[4] MATĚJOVÁ, L., Kočí, K., RELI, M., ČAPEK, L., HOSPODKOVÁ, A., PEIKERTOVÁ, P., MATĚJ, Z., OBALOVÁ, L., WACH, A., KUŚTROWKSI, P., KOTARBA, A.: Preparation, characterization and photocatalytic properties of cerium doped TiO_2: On the effect of Ce loading on the photocatalytic reduction of carbon dioxide. *Applied Catalysis B: Environmental* 152–153 (2014) 172–183.

[5] LIANG, Ch.-H., LI, F.-B., LIU, Ch.-S., LÜ, J.-L., WANG, X.-G.: The enhancement of adsorption and photocatalytic activity of rare earth ions doped TiO_2 for the degradation of Orange I. *Dyes and Pigments* 76 (2008) 477–484.

Determination of physical properties of liquids via acoustic levitation

Judith Kremer

Chair of particle technology, Ruhr-University Bochum, Germany

Email: kremer@fvt.rub.de

The knowledge of physical properties is essential in many industrial applications. But the determination of physical properties like surface tension, viscosity and density of fluids is challenging, especially under high pressure. The aim of this project is to prove the suitability of the acoustic levitation as a measurement method for these thermophysical properties of liquid substances under ambient conditions and under high pressure.
Currently there are no measurement methods that can measure surface tension, viscosity and density without any contact to a surface. The measurement of these physical properties is challenging at ambient pressure, in high pressure systems it is even more complicated. Furthermore, there is no equipment which can determine these properties within only one measurement.
The principle of levitation can be used to avoid any contact between the liquid sample and a surface. The different levitation techniques are divided into groups after their underlying physical principles. There are for example the magnetic, electrostatic or the acoustic levitation. One advantage of the acoustic levitation is that the substance does not need to fulfill special requirements. Another advantage is that the volume of the levitated sample is very small (5 to 10 μl). Thus the acoustic levitation is a promising technique especially for expensive and/or rare materials.
The principle of acoustic levitation is shown in figure 1.

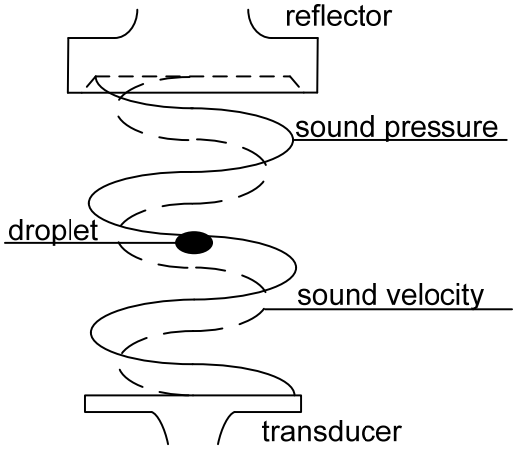

Figure 1: Principle of acoustic levitation [1]

An ultrasonic standing wave field is created when an ultrasonic wave emitted by a transducer is reflected by a coaxial reflecting surface, the reflector. The ultrasonic waves interfere with each other if the distance between the transducer and the reflector is an integer multiple of half the wavelength. Because of the varying magnitude of the sound pressure and the sound particle velocity there are positions where the pressure is at its minimum and the sound particle velocity

is at its maximum. A small solid or fluid object can be placed contactless in these potential wells because the acoustic force overcomes the gravity force in these positions. The forces are the axial force caused by the sound pressure and the radial force caused by the sound particle velocity. Their ratio is 5:1, so a liquid drop is deformed to an oblate rotational ellipsoid. Furthermore the center of a levitated probe deviates slightly from the pressure node because of gravity.

The levitated droplet can be manipulated contactless through a modulation of the ultrasound carrier signal. The droplet response to the modulation is droplet shape oscillations. The center of the drop is fixed below the pressure node and only the shape of the droplet oscillates. The droplet is recorded with a high speed camera at 1000 fps. For the determination of the surface tension the drop is exited to axisymmetric oscillations in the quadrupole mode. That means that the drop shape varies between an oblate and a prolate shape (Mode l = 2 and m = 0). In figure 2 an oscillating ethanol droplet in the quadrupole mode is shown. On the left side the droplet forms the maximum oblate shape and on the right the maximum prolate shape.

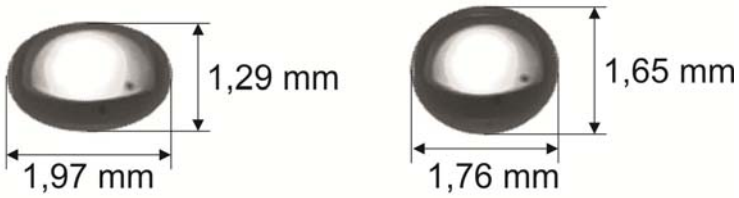

Figure 2: Oblate and prolate shape of an oscillating ethanol drop

The surface tension σ is calculated with the frequency ***f*** of the drop shape oscillations, the density of the liquid ***ρ*** and the equatorial radius ***a*** of the drop [2].

$$\sigma = \frac{(2\,\pi\,f)^2\,\rho\,a^3}{8} \qquad (1)$$

The frequency of droplet shape oscillations depends on the equatorial radius of the drop and the liquid (figure 3). The experimentally determined oscillation frequencies of ethanol droplets are compared to theoretical values for the oscillation frequency calculated with equation 1.

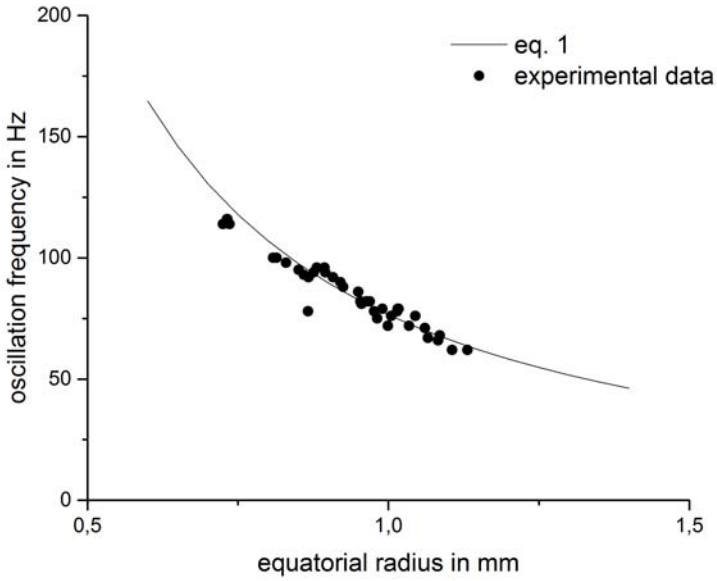

Figure 3: Frequency of droplet shape oscillations for an ethanol drop levitated in air

The experimentally observed oscillation frequency is in good agreement to the theoretical values of equation 1. The frequency of drop shape oscillations decreases with increasing equatorial radius. It is a potential function of the form $f = C \cdot a^{-1,5}$ with the equatorial radius ***a*** of the drop and the constant ***C***. The constant ***C*** depends only on the liquid. The overall uncertainty is $\pm$ 6 %. The viscosity is determined through the damping of these oscillations when the modulation signal is switched off.

Furthermore the density of the levitated sample can be determined by the voltage needed to levitate the sample and a reference material. A drop of the reference material (e.g. water) is placed in a pressure node of the standing wave. Afterwards the amplitude of the levitation signal is reduced until the drop falls out. Then the same is done with a drop of the sample material with the same position of the reflector. The density can be determined with the density of the reference material and the ratio of the voltages needed to levitate the drops. Density determination via acoustic levitation gives results that are in very good agreement to the values obtained with conventional methods for the determination of density.

[1] D. Borosa, S. Kareth, M. Petermann, *Chem. Ing. Tech.*, 2012, 84, 145-148.

[2] C. L. Shen, W. J. Xie, B. B. Wei, *Sci. China Phys. Mech. Astron.*, 2010, 53, 2260-2265.

Diffusivity of water encapsulated in fat particles through structured 3-d surfaces solid fat/liquid water

Rebecca Scholz

Chair of Process Technology, Ruhr-University Bochum, Germany

Email: rscholz@vtp.rub.de

The aim of this project is to understand the release from encapsulated microparticles. These multiphase release systems are under investigation in a joint research approach within the RESOLV cluster of excellence which focuses on solvation science. In general, the capsules consist of at least two different substances, the core and the shell material. The objective is to produce stable microcapsules with triglyceride as shell and water as core material. The microcapsules can be produced via different techniques: the PGSS (Particles from Gas Saturated Solutions) process, the HPH (High Pressure Homogenizer) and a rotor-stator system. The last two technologies are based on the melt dispersion technique. In figure 1 a scheme of the generation of the capsules in lab scale is shown. The first step includes the preparation of a water-in-oil-emulsion (W_1/O). The second step is the production of a double emulsion (W_1/O/W_2). The capsules are generated after shock cooling of this double emulsion by solidification of the shell material. This is obtained by adding iced water.

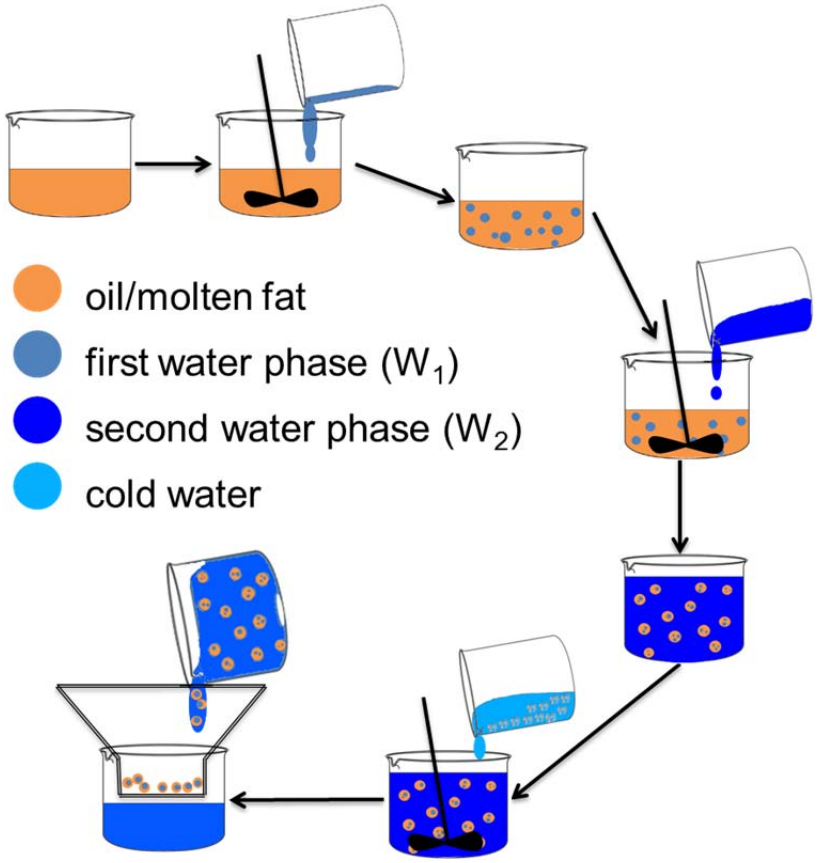

Figure 1: Schematic drawing of the process for capsule generation in lab scale. First the preparation of first emulsion (W_1/O), second the preparation of double emulsion (W_1/O/W_2), and then solidification and filtering.

These capsules are characterized related to size, morphology and macroscopic characterization of the release properties, e.g. weight loss measurements. The size of the capsules should range in this project between 1 and 100 µm. The properties morphology, stability and formation of the capsules are influenced by the material of the core and the shell, the temperature of the cooling water and the additives, more precisely the type and the concentration of the emulsifier or stabilizer. As additives polyvinyl alcohol, different types of Span (lipophilic emulsifier) and Tween 80 (hydrophilic emulsifier) are used. The dependency of the stability of the capsules respectively the release of water through the shell material via diffusion/evaporation or via triggered disintegration of the capsules is investigated as function of the type of additives.

In a first attempt the rotor-stator system was used for encapsulation of yellow fluorescent protein (YFP) [1]. YFP is used as tracer to visualize the release of the substance. First, a water-in-oil (W/O) emulsion is obtained consisting of the core material, YFP in a buffer solution, and a hard fat, a mixture of mono-, di- and triglycerides, as shell. The d_{50} of these particles is 130 ± 14 µm with a quite narrow particle size distribution (span of 1.4 ± 0.1). In one production step two different types of capsules are generated, the core-shell type and the matrix type. The temperature dependent release of the protein is measured with a novel thermal microscopy technique, a method which combines temperature jumps with fluorescence imaging (figure 2). The temperature jumps are realized with an infrared laser and the images are taken with a high speed microscope [2]. These measurements are performed in the collaboration with the group of Ebbinghaus (Ruhr-University Bochum, Germany).

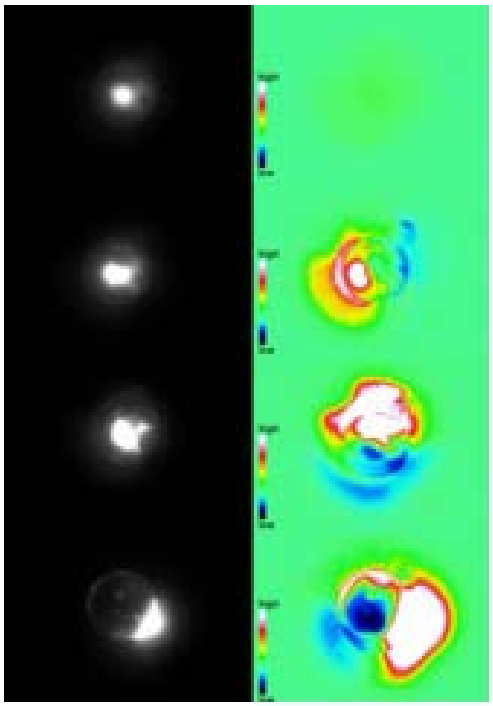

Figure 2: Fluorescent images taken during the heating experiment. The fluorescent protein is released after melting the shell material.

The additives in the capsules are Tween 80, Span 80 and PVA. PVA increases the viscosity of the outer water phase. Span consists of sorbitan esters with different alkyl groups. It is possible to find a range of Span with different properties like the HLB[1] value. The encapsulation

[1] The HLB (Hydrophilic-Lipophilic Balance) value hints the solubility in different phases.

efficiency (EE) of the capsules prepared with different types of Span is measured. The different emulsifiers with their properties are compared in table 1. The core material is a 10 wt% NaCl solution, the shell material is Witepsol W31. The concentration of the emulsifiers is set to 5 wt% referring to the fat. The encapsulation efficiencies are measured via conductivity, so the tracer in these measurements is NaCl. The capsules are molten and the concentration of the salt in the water is measured with an electrical conductivity meter (Cond 3310 SET 1 from WTW).

Table 1: Comparison of studied emulsifiers with different HLB values and the results of their encapsulation efficiency and their size.

Emulsifier	**Chemical identity**	**HLB**	**EE in %**	**d_{50} in µm**
Span 20	Sorbitan monolaurate	8.6	47 ± 16	145 ± 23
Span 65	Sorbitan tristearate	2.1	64 ± 4	119 ± 19
Span 80	Sorbitan monooleate	4.3	45 ± 7	206 ± 60

The highest encapsulation efficiency is obtained by using Span 65 as emulsifier. These results are compared to the 2-dimensional measurements by the group of Tolan to explain the dependency between the type of emulsifier and the encapsulation efficiency. They figured out that Span 60 and Span 65 array in a homogenous layer at the air/water interface. In contrast, Span 80 and Span 85 form islands at the interface. So, the structure of the emulsifier layer between the core material and the shell material has an influence on the encapsulation efficiency. The denser the layer of the emulsifiers the higher is the amount of the encapsulated material.

The collaborating groups of this project focus on the temperature dependent diffusion of water in the 3-dimensional system. The behavior of the already mentioned additives and their properties at a 2-dimensional interface between water and fat phases are analyzed via Langmuir Trough, Brewster angle microscopy and interfacial rheology. The geometric structure of these surfaces is also studied via synchrotron experiments. The results are compared with the outcomes of the measurements with a spectral ellipsometry which measures the sorption of water at a dodecanethiol (DDT) self-assembled monolayer (n = 12) as 2-dimensional model surface. This model surface has a long alkyl chain like the dominated component triglyceride (65-80 %) of the used fat (Witepsol W31). The DDT surfaces will be also studied with the new developed nanobalance to measure mass changes. Gravimetric measurements of the capsules with the nanobalance are also planned to study the mass change over time in a well-defined environment. The idea is to get information about the diffusion and evaporation of the water encapsulated in a fat.

[1] T. Vöpel, R. Scholz, L. Davico, M. Groß, S. Büning, S. Kareth, E. Weidner, S. Ebbinghaus, *Chem. Comm.*, 2015, 51, 6913-6916.

[2] S. Ebbinghaus, A. Dhar, J. D. McDonald, M. Gruebele, *Nat. Methods*, 2010, 7, 319-323.

Vapour pressure measurements with a magnetic suspension balance

Ricarda Kendler

Chair of Particle Technology, Ruhr-University Bochum. kendler@fvt.rub.de

The vapour pressure is the pressure of a vapour in thermodynamic equilibrium with its condensed phase, solid or liquid. For pure substances the vapour pressure only depends on the temperature. The OECD guideline for the testing of chemicals describes eight methods to measure the vapour pressure. Each method is valid for a different pressure range. These methods are:

- the dynamic method
- the static method
- the isoteniscope method
- the effusion method (vapour pressure balance)
- the effusion method (knudsen cell)
- the effusion method (isothermal thermogravimetry)
- the gas saturation method and
- the spinning rotor method

Presently, no measuring method exists to measure the vapour pressure over a wide range of pressure. Depending on the material and the temperature, the vapour pressure varies between some mPa for substances like benzoic acid and several Pa for substances like limonene or toluene. Thus there is a need for a system which can measure the vapour pressure of almost all substances, pure or mixtures, in a wide range of pressure. The aim of the presented research topic is to develop and to build a prototype which fulfils this requirement. This will be realized with a modular system based on a magnetic suspension balance (MSB). Every module uses a different measuring method. The development of this measuring system is carried out in cooperation with Rubotherm, the producer of the magnetic suspension balance.

The main component of the measuring system is the MSB. This balance enables a contactless weighing of the sample's mass in a wide range of pressure and temperature conditions. The MSB consists of a microbalance and a measuring cell containing a sample carrier with the sample to be investigated. Both sample and balance are connected by a magnetic coupling. As the microbalance and the sample are separated from each other, so the conditions inside the measuring cell don't disturb

the microbalance. Fig. 1 shows a schematic image of the MSB. Two positions of the balance are available: Zero point (ZP) and measuring point (MP). In the zero point position the electromagnet only holds the suspension magnet which consists of the permanent magnet, the sensor core and a device for decoupling the measuring load in suspense. The sample is decoupled from the balance. In the measuring position the suspension magnet and the sample are suspended by the electromagnet. This enables a permanent automatic taring and calibration during a measurement and leads to a highly precise measurement of a sample's load, especially for long term measurements.

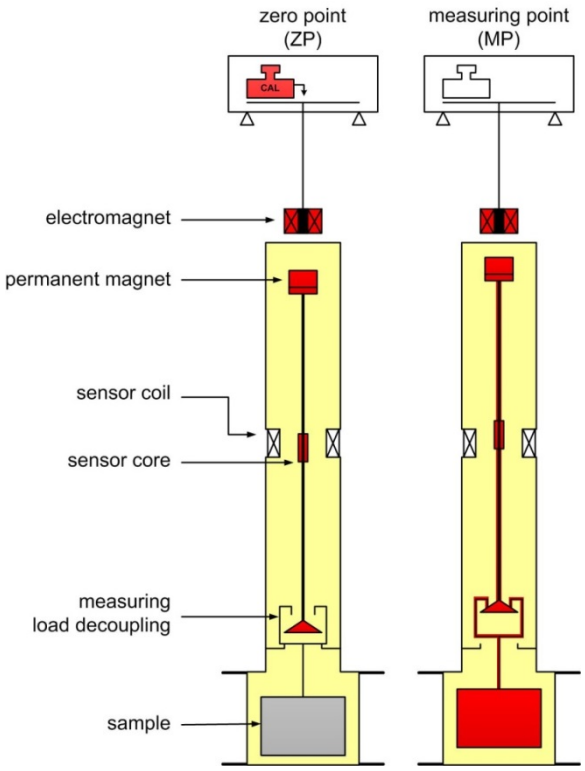

Fig. 1. Schematic image of the two positions of the MSB

Inside the measuring cell a static or a flowing atmosphere as well as an inert gas atmosphere can be set while pressure and temperature are adjustable parameters.

The measuring cell is surrounded by a double jacket that is connected to a thermostat for heating or cooling. For adjusting different atmospheres and pressures inside the cell, a gas dosing system is connected to the MSB. In case of a flowing atmosphere the inert gas, here nitrogen, flows top down or bottom up through the cell. Different modes of operation can be selected in dependency of the desired measuring method. For example, the Knudsen method needs a vacuum inside the cell and the isothermal thermogravimetry a pressure of one atmosphere.

In the beginning of the research, the measuring methods which can best be integrated to the MSB were selected. The first method to be tested in the MSB is the isothermal thermogravimetry and is described in the following: A simple cylinder as a sample container was used. The nitrogen flowed top down through the cell with 10 ml/min.

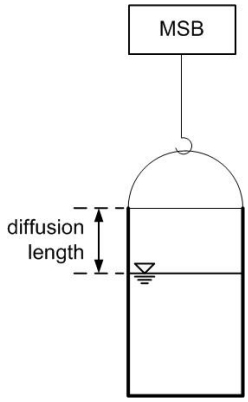

Fig. 2. Schematic image of the sample container

The nitrogen is not pre-saturated with any substance and the vapour of the substance in the cylinder starts diffusing into the surrounding atmosphere. The vapour pressure was calculated under the assumption of a diffusion-controlled evaporation through a stagnant gas layer. The concentration at the sample's surface equals the equilibrium concentration at the prevailing temperature. At the mouth of the container the sample concentration is negligible. So the length of the diffusion layer reaches from the surface of the sample to the mouth of the container. This diffusion length changes with time. Convective mass transfer was also neglected, because the flow pattern of the inert gas is complex and unknown. The binary diffusion coefficients are estimated using the empirical Fuller method. [2] Experiments were made with ethanol and the results are shown in fig. 2.

As expected, the measuring vapour pressure increases with increasing temperature and the experimental values are below the literature values, because convective mass transfer was ignored.

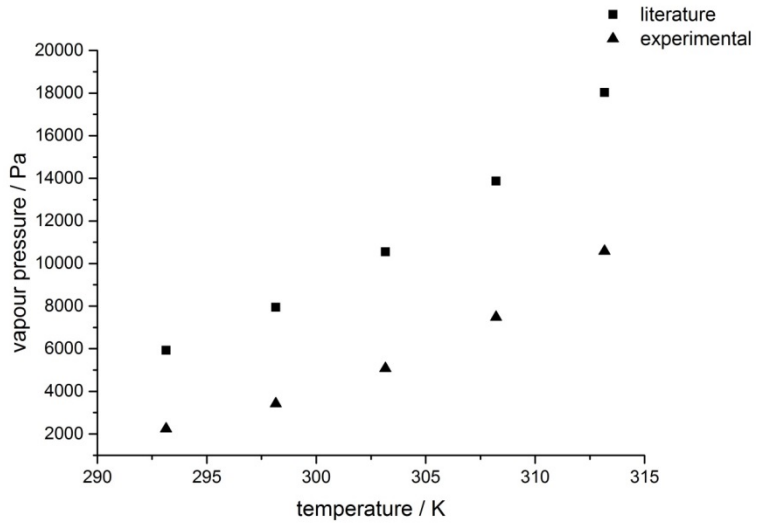

Fig. 3. Comparison of vapour pressure values estimated from experimental data and using literature values calculated with ThermoFluids

In the next step, a new sample container with improved properties will be built. The chamber will consist of a cylindrical container with a capillary at the bottom. For these experiments the inert gas flows bottom up through the cell. The vapour pressure can be calculated by the formula for one dimensional diffusion through a stagnant gas layer.

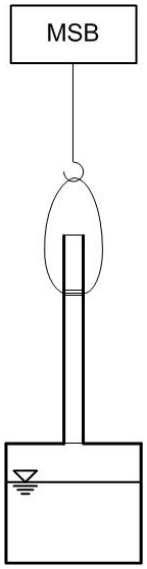

Fig. 4. Schematic image of the new sample container with a capillary

References

[1] OECD, Test No. 104: Vapour pressure, OECD guidelines for the testing of chemicals, Section 1, OECD Publishing, Paris, 2006.

[2] E. L. Cussler, Diffusion: mass transfer in fluid systems, 3rd ed., Cambridge University Press, New York, 2009, p. 123.

Modification of $CuWO_4$ Photoelectrodes for Water Splitting

Olga Melchaeva, Fraunhofer UMSICHT, 6047 Oberhausen

The depletion of fuel stocks and adverse impact on the environment indicate the necessity of alternative sources of clean energy. Solar energy is so vast that it exceeds the current global human energy consumption (1.6 x 10 TW in 2010)[1, 2] by roughly four orders of magnitude. It is an attractive and abundant natural source with about twice as much energy as will ever be obtained annually from all of the Earth's non-renewable resources of coal, oil, natural gas, and mined uranium altogether.[3, 4] One of the most promising approaches to the energy issue consists in collecting and storing solar energy in chemical bonds through photosynthesis. Therefore, this research was focused on modification and optimization of photoelectrodes for water splitting and simultaneous current generation.

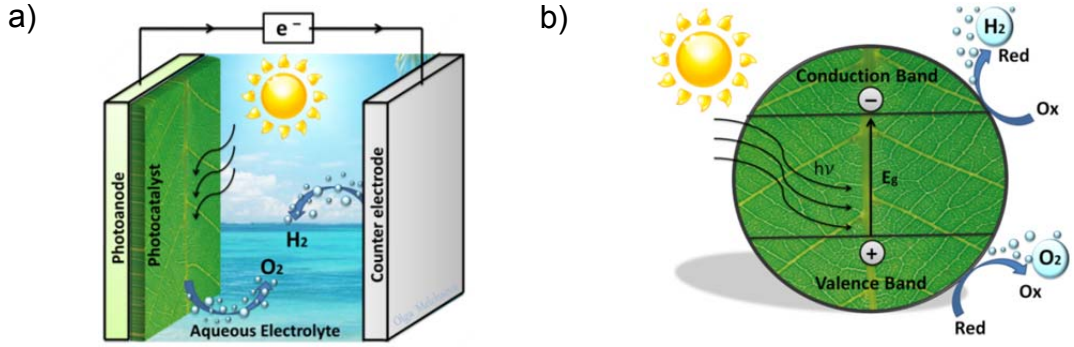

Figure 1: Illustration of (a) photocurrent generation and subsequent water splitting in photoelectrochemical cell (PEC) consisting of a photoanode and a metal cathode; (b) charge separation inside of the photocatalyst (semiconductor).

The solar energy was harvested by the use of photoelectrochemical cells (PEC) due to their relative fabrication simplicity, separate containers for H_2 and O_2 generation, economic viability and potentially high efficiency. Working principal of the PEC devices and semiconducting materials is depicted in Figure 1. The semiconductor in PEC was immersed into aqueous solution of an electrolyte. When a semiconductor is irradiated by light with energy higher than the bandgap energy ($hv > E_g$), electrons are excited from the valence (VB) to the conduction (CB) band, leaving the positive “holes” in CB.[5] These photogenerated charge carriers are transferred to the surface active sites and simultaneously drive reduction and oxidation of the aqueous electrolyte. The basic reaction for water decomposition is as follows:

$$2H_2O \xrightarrow{hv} 2\,H_2 + O_2$$

Copper tungstate ($CuWO_4$) was chosen as an attractive material for water splitting. It is an n-type semiconductor with a small bandgap of 2.2 – 2.4 eV, which allows harvesting a large portion of visible light (~564 nm).[6] It shows high stability over long-term illumination in aqueous electrolytes and high Faradaic efficiency of oxygen generation from water, making it a promising photocatalyst.[7]

However, despite all the advantages, $CuWO_4$ exhibits limitations associated with low mobility of charge carriers provoking high recombination rates. Therefore, in order to overcome this problem, $CuWO_4$ was modified following two strategies: *doping* with metal ions Cu^{2+}, Zn^{2+}, Co^{2+}, Sn^{2+}, Pb^{2+} and La^{3+} and *complementing with another wide-bandgap semiconductors* like TiO_2 and SnO_2. Besides, different precursors, treatment conditions, methods of photocatalysts synthesis, optimal layer thickness, back- and frontside irradiation and different electrolyte solutions were tested.

Experimentally it was found that $CuWO_4$ films obtained from precursors copper (II) acetylacetonate and tungsten isopropoxide exhibited the highest photoelectrochemical properties and therefore were used throughout this project. Concerning different application methods such as doctor blade and dip-coating, the latter was proven to be an attractive technique for film deposition due to the controllability of layer thickness, which increases with the amount of dip-coatings. Optimization of the temperature treatment and layer thickness of $CuWO_4$ photoanodes has shown that annealing at 450 °C for 2 hours and 15 times dip-coating result in higher photocurrent density (171 $\mu A/cm^2$ at 380 nm), incident photon-to-current efficiency (IPCE) (5.1% at 380 nm) and greater photocatalytic activity (153 $\mu mol/dm^3$ of O_2 generation within 3.8 h). Photocurrent activity of the $CuWO_4$ electrodes was ranging from 300 to 550 nm. Additionally, the chemical stability of electrodes was tested in two electrolyte solutions phosphate and borate buffers at pH 7.9, where the latter has shown significantly lower photocurrent degradation under sunlight irradiation. Analysis of back- and frontside irradiation showed higher photocurrent in case of the former, due to the easier diffusion of holes to the electrolyte and better transport of electrons to the back contact of the underlying FTO glass substrate.

When the right parameters of $CuWO_4$ synthesis, optimal irradiation side and, electrolyte solution were established, the electrodes underwent modification. According to the *first strategy*, doping with metal ions was meant to improve electron mobility by introduction of impurities and adjustment of the electronic structure of the conduction band of

$CuWO_4$. According to ref. [8], The CB of $CuWO_4$ contains the empty Cu $d_{x^2-y^2}$ states, which are responsible for the low electron mobility, due to the additional transfer of electrons from Cu d_{z^2} to the empty states of Cu and p-states of neighboring oxygen atoms.[8, 9] Thus, the best results were achieved by La-doped $CuWO_4$ electrodes. The photocurrent density was increased by maximum of 35 $\mu A/cm^2$ ranging from 330 to 470 nm (Figure 2 a), IPCE efficiency and oxygen evolution were enlarged on 1% and 4%, respectively. UV-Vis diffuse reflectance spectrum data of La-doped $CuWO_4$ electrodes showed the shift of absorption edge from 543 to 520 nm and broadening of the bandgap from 2.28 to 2.38 eV in comparison to the un-doped $CuWO_4$ samples, respectively. It means that the electronic structure of $CuWO_4$ was altered, which improved the electron mobility and resulted in higher photocurrent and efficiency of the electrodes.

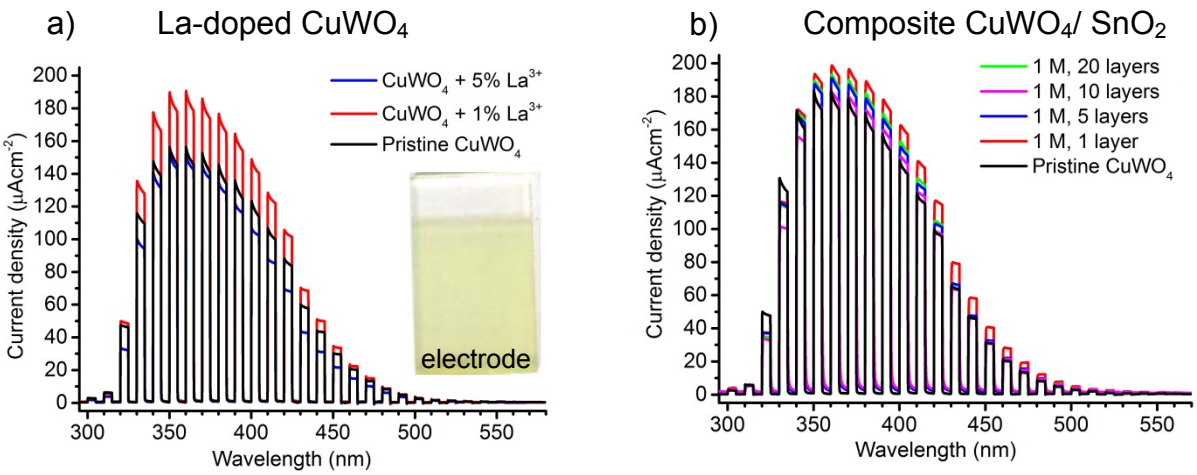

Figure 2: Photocurrent measurements (a) La-doped $CuWO_4$ electrodes (dopant concentration of 1 and 5 mol%); (b) $CuWO_4/SnO_2$ composite electrodes (1 M SnO_2 solution concentration with amount of layers: 1, 5, 10 and 20 times). The measurements were recorded in borate buffer (pH 7.9, 0.1 M) under intermittent monochromatic backside irradiation. Applied potential was 1.17 V vs. RHE.

According to the *second strategy*, $CuWO_4$ was implemented with *a wide bandgap metal oxide* with high carrier transport properties, like TiO_2 or SnO_2. (Figure 3 a) Both of the materials are n-type semiconductors, exhibit efficient electron mobility and have a wide bandgap of 3.2 V (390 nm)[6] and 3.6 eV (~335 nm)[10], respectively. In $CuWO_4/TiO_2$ and $CuWO_4/SnO_2$ composites the materials are meant to complement each other. $CuWO_4$ supposed to harvest visible light and inject the electrons to complementing semiconductor, while TiO_2 or SnO_2 collect electrons and enhance their mobility. Among composites only $CuWO_4/SnO_2$ electrodes have shown a slight improvement of $CuWO_4$

photoelectrochemical properties. To find the optimal thickness, SnO_2 was synthesized from the precursor solution with different concentrations and by means of different amount of layer deposition. Composite electrodes with SnO_2 obtained from 1M solution and one time dip-coating have shown the improvement of photocurrent density by maximum of 20 $\mu A/cm^2$ in the range from 350 to 490 nm (Figure 2 b) and 0.5 % increase of IPCE efficiency. This proves the electron transfer from $CuWO_4$ to SnO_2 and supports the idea of complementary mechanism, where $CuWO_4$ acts as a visible light absorber and SnO_2 as a scaffold material (Figure 3 b).

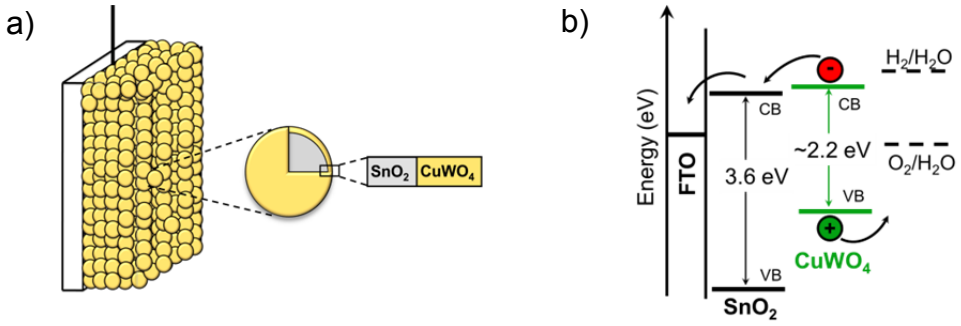

Figure 3: (a) Schematic representation of $SnO_2/CuWO_4$ composite system. SnO_2 nanoparticles are enveloped by a thin layer of $CuWO_4$; (b) energy diagram of electron transfer from $CuWO_4$ to SnO_2. Conduction band (CB) of $CuWO_4$ is high enough to inject the electron to CB of SnO_2.

To sum everything up, modification of $CuWO_4$ via *doping* with Cu^{2+}, Zn^{2+}, Sn^{2+} and La^{3+} metal ions and by *combination* with SnO_2 semiconductor has shown a moderate improvement of photoelectrochemical properties. Therefore, further investigations are needed to evaluate the full promise of these methods for the improvement of $CuWO_4$ photoanodes.

[1] T. Hisatomi, J. Kubota, K. Domen, *Chemical Society Reviews* **2014**, *43*, 7520-7535.
[2] *BP Statistical Review of World Energy June* **2013**, BP Statistical Review of World Energy, BP p.l.c, 1 St James's Square, London, SW1Y 4PD, UK.
[3] W. A. Hermann, *Energy* **2006**, *31*, 1685-1702.
[4] P. Würfel, *Physics of Solar Cells: From Principles to New Concepts*, **2007**.
[5] R. Beránek, PhD thesis, Friedrich-Alexander-Universität Erlangen-Nürnberg **2007**.
[6] K. J. Pyper, J. E. Yourey, B. M. Bartlett, *The Journal of Physical Chemistry C* **2013**, *117*, 24726-24732.
[7] N. M. Gaillard, *Electrochemical Society* **2013**.
[8] M. V. Lalić, Z. S. Popović, F. R. Vukajlović, *Computational Materials Science* **2012**, *63*, 163-167.
[9] S. K. Pilli, T. G. Deutsch, T. E. Furtak, L. D. Brown, J. A. Turner, A. M. Herring, *Physical Chemistry Chemical Physics* **2013**, *15*, 3273-3278.
[10] Z. Chen, J. K. L. Lai, C. H. Shek, H. Chen, *Journal of Materials Research* **2003**, *18*, 1289-1292.

Investigation of a Cationic Nickel Diimine Complex for Ethylene Polymerization under High Pressure Conditions

M. Balyschewa, Technische Universität Darmstadt, Ernst-Berl-Institut für Technische und Makromolekulare Chemie, Germany;

M. Busch, Technische Universität Darmstadt, Ernst-Berl-Institut für Technische und Makromolekulare Chemie, Germany

In industry there are two relevant modes to polymerize ethylene, free radical polymerization under high pressure and catalytic polymerization under medium up to high pressure. These provide products of dedicated different microstructure, what has a significant impact on physical and mechanical properties of the polymer. The free radical polymerization of ethylene in a high pressure process (1500-3000 bar) provides a product whose microstructure consist of random distributed short (SCB) and long (LCB) chain branching. LCB affect the rheology and make the polymer more flexible, while SCB cause low densities and crystallinities. Therefore the product of the high pressure process is known as *Low Density Polyethylene* (LDPE).

The second industrially relevant mode for ethylen polymerization is the coordinative polymerization by transition metal catalysts at medium pressure (14-69 bar). Industrially heterogeneous Ziegler-Natta- and homogeneous Metallocene catalysts are used to polymerize ethylene. The products microstructure is exclusively linear with practically no branching. Due to the lack of SCB it has higher densities than LDPE and wherefore referred as *High Density Polyethylene* (HDPE).

Novel homogeneous catalysts are able to produce SCB branched polyethylene. In 1995 Brookhart et al.[1] reported first on the discovery of this new class of catalysts for the polymerization of ethylene. They are based on cationic palladium(II) and nickel(II) complexes with bulky substituted diimine ligands. They are capable to generate high molecular weights and randomly distributed SCB. This amorphous and semicrystalline products constitutes a new class of polyethylene, as it is far more highly branched (up to 100 per 1000 C-Atom) than *Low Density Polyethylene* (ca. 25 per 1000 C-Atom). In addition the microstructure generated by the nickel(II) complex shows a dependency toward temperature, pressure (1-4 bar) and the catalyst structure. For example increasing temperatures lead to higher branching degrees, increasing pressure causes the opposite effect at unchanged yield and molecular weight.

Following on this observation we will polymerize ethylene with an cationic nickel(II) diimine Brookhart catalyst at different high pressure (up to 2000 bar) and temperature (up to 200 °C) conditions to examine those impact on the microstructure of the product. The experimental setup for this study is a continuous high pressure polymerization plant. The continuous stirred high pressure autoclave has an internal volume of 15 mL and is constructed for pressures up to 2500 bar and temperature up to 300 °C.

[1] M. Brookhart, *Journal of the American Chemical Society*, **1995**, 117, 6414-6415.

Modelling of High Pressure Polymerizations in Tubular Reactors

Kristina Zentel, Markus Busch, Technische Universität Darmstadt, Darmstadt/Germany

Polyethylene is one of the most important commodity polymers of our time. Polyethylene production almost reached 300 million tons in 2013, which represents nearly 30% of the overall plastic production. It is this popular because it is not only cheap but offers many areas of application at the same time. Those are not only packaging, bags and pipes, but also special applications such as isolation materials for high voltage components or medical equipment.

Depending on the desired product properties, a different type of polyethylene can be chosen as material. The three main products of polyethylene are LDPE (Low Density Polyethylene), HDPE (High Density Polyethylene) and LLDPE (Linear Low Density Polyethylene). Although consisting of the same monomer, ethylene, these products possess different physical properties. They vary in their density, melting temperature, degree of crystallinity and mechanical behavior. These differences in the macroscopically observed physical properties are attributed to the microscopic structure of the macromolecules, which is strongly influenced by the synthesis route (free radical or catalytic polymerization), the reaction conditions (high or low pressure), the reactor type (tubular reactor or autoclave) and the addition of comonomers and/or CTA (Chain Transfer Agent).

LDPE was first produced by the ICI (Imperial Chemical Industries) in 1939 at a temperature of 170°C and at a pressure of 1900 bar. Nowadays this free radical polymerization process is typically operated under pressures up to 3000 bar and at temperatures between 100°C and 300°C. These exceptional process conditions result in high investment and production costs. Low pressure catalytic processes pose a lucrative alternative to the high pressure process. They yield HDPE and LLDPE, which do not possess the special rheological properties of LDPE, which are highly desired for certain processing steps. Whereas HDPE exists of linear macromolecules, LLDPE exhibits short chain branches due to copolymerization with higher α-olefines such as butene, hexene or octene. LDPE possesses short chain branches (SCBs), which are created by an intramolecular backbiting. Furthermore it contains long chain branches (LCBs), which are introduced into the macromolecule by intermolecular transfer reactions. These LCBs are responsible for the extraordinary properties of LDPE.

As the high pressure polymerization of ethylene is a process at the edge of technical feasibility, it is of utmost importance to improve the existing process. Improvements are necessary both from an economic and from an ecologic point of view, for example concerning the high energy demand or desired product qualities. As any tests in industrial world-scale plants are almost unaffordable and experiments in miniplants still costly, simulations with a predicative nature are a welcome, cost-effective, but reliable alternative. The mathematical prediction of process parameters for the LDPE-synthesis, for instance conversion, molecular weight distribution and branching, has been studied and refined since the late 1960s. By now the process

simulation for LDPE synthesis poses a crucial tool for the LDPE-process development and optimization. But for the conduction of reliable and precise process simulations it is essential to have a very profound knowledge and understanding of the process itself, its thermodynamics and kinetics and of course of the structure-properties relationship of the resulting polymer. Therefore a uniform set of parameters is essential, which can describe the polymerization reaction independently of reactor type and process. However, this proves to be a highly demanding task as numerous parameters have to be known sufficiently precise within a complex reaction network and under extreme process conditions. This is why variable parameters are still necessary in the current simulation models in order to obtain good agreement between calculation and plant data [1]. For tube reactors these parameters are e.g. the initiator efficiency and the thickness of the fouling layer inside the reactor.

My area of investigation mainly deals with the modelling of the high pressure polymerization of ethylene in tubular reactors. Compared to autoclaves tubular reactors exhibit a higher surface-to-volume ratio, which makes cooling more effective and thus results in higher conversions. Moreover investment costs are lower, because the reactors, which reach lengths up to 2 km, are assembled of standardized double pipe modules.

The reactor itself can be divided into several reaction zones. At the beginning of the first zone ethylene and CTA are fed into the reactor and initiator is added to the process in order to start the polymerization. The temperature passes through a maximum, as the mixture is cooled through the countercurrent cooling in the annular gap. At the beginning of each of the following reaction zones more initiator is added in order to restart the polymerization. Cold gas injections along the reactor axis can also achieve maximum cooling and conversion.

Typical initiators for the LDPE process are organic peroxides, such as di-*tert*-butyl peroxide (DTBP), but molecular oxygen is also being applied. Oxygen is particularly interesting as it exhibits both initiating and inhibiting properties, so that unusually shaped temperature profiles are observed. E. Neuhaus developed a reaction scheme, which is able to describe oxygen-initiated polymerizations in tubular reactors quite satisfactorily [2].

The existence of variable parameters as well as systematic discrepancies within the reactor models give reason for further investigations. In order to identify and overcome the knowledge gaps a systematic sensitivity analysis of the existing model concerning possible faulty parameters is the reasonable approach.

In a first approach the fundamentals, such as the thermo-physical properties, which serve as the basis of the polymerization model, have been revisited in my masters thesis. For the simulation these properties are the density, heat capacity, viscosity and heat transfer coefficient of ethylene, LDPE and the reaction mixture. These data have to be available in dependence on temperature, pressure and composition, respectively. Whereas the density, the heat capacity and the thermal conductivity primarily influence the heat balance of the model, the viscosity of the reaction mixture also influences the kinetics directly. Literature on these properties for the pure

components under process conditions is scarcely available and mostly dates back to the 1950s and 60s [3]. Furthermore it often contains extrapolations and was analyzed with outdated mathematical methods. Moreover it becomes evident that some of the authors obtain differing values for the thermo-physical properties at a given temperature and pressure. Consequently the discrepancies also within the model reach up to several percent.

The next step would be to have a closer look at the complex reaction network of the ethylene polymerization again. In order to describe this polymerization sufficiently precise, one has to consider more than the ideal kinetics of the free radical polymerization. These are initiation, propagation and termination by disproportionation and recombination. Moreover transfer to low molecular species, such as the monomer and the CTA has to be taken into account. These reaction steps terminate growing chains and thus reduce the molecular weight. Intramolecular transfer reactions via backbiting account for SCBs, whereas intermolecular transfer reactions create secondary radicals. These secondary radicals can either undergo a β-scission, which splits the chain into two parts, or form a LCB by continuing chain growth. As already indicated these LCBs are especially important for the unique rheological properties of LDPE. However, there are indications that this reaction step cannot yet be described completely by the present model. There might exist a not negligible dependence of the kinetic coefficient on monomer conversion. The approach to further investigate this matter has to be designed carefully.

In order to get a deeper understanding of the structure-properties relationship of LDPE, the mean values of microstructural properties (e.g. average long and short chain branch densities) as obtained by deterministic simulations prove to be insufficient. But the conduction of stochastic Monte-Carlo simulations generates individual macromolecule samples with an exact polymeric topology. These samples contain much more detailed information concerning the polymeric microstructure of LDPE than any deterministically achieved results. As a pure stochastic simulation with a sufficient accuracy requires an enormous amount of time, the hybrid concept developed by E. Neuhaus can be applied here [2]. Heat and pressure balances as well as reaction frequencies are calculated deterministically with the simulation tool Predici in the first step. In a next step this data set is used in a stochastic algorithm to simulate a certain number of distinct macromolecules with completely known microstructure one after another. Evaluating these results hopefully helps to identify new ways of how the LDPE process can be further improved and of how desired product properties can be controlled.

[1] T. Herrmann, *Dissertation,* Darmstadt **2011.**
[2] E. Neuhaus, *Dissertation*, Darmstadt **2014**.
[3] G. Luft, R. Steiner, *Chemiker-Zeitung* **1971**, 95 (1), 11-15.

Modelling of technical reactors for the production of ethylene copolymers.

Sascha Griebenow, Markus Busch, Technische Universität Darmstadt.

The free radical high-pressure polymerization of ethylene has been used in industry for years to produce low-density polyethylene (LDPE) and ethylene copolymers. These processes are characterized by high reaction temperature (150 – 300 °C) and pressure (1000 – 3000 bar). The reaction mixture behaves as a supercritical fluid, with polymer soluble in the unreacted monomer under most operating conditions. Both stirred autoclave reactors and tubular reactors are commonly used in the industry. It is known that polymers manufactured by these processes differ in their molecular architecture and many of the important application properties. Polymers produced in autoclave reactors are more hazy than those produced in tubular reactors and suitable for extrusion coating and molding applications. The simulation of existing industrial reactors is an important tool to understand the processes inside the reactor. This knowledge helps to optimize industrial facilities or to plan the construction of new industrial reactors. Without cost- and time-intensive experiments the simulation allows to investigate product-oriented recipes in advance. Additionally the knowledge of the processes inside the reactor results in a better risk assessment and thereby leads to an increase in safety.

The aim of this scientific work is the development of a model. It should be able to describe a free radical high pressure copolymerization in a technical autoclave reactor. Beside the simulation another target is to evolve a gel permeation chromatography (GPC) method to measure the molecular weight distribution and the composition of the copolymer as a function of the elution volume.

To detect the molecular weight distribution a light scattering detector (LS) is used and is combined with an infrared detector (IR) which detects the composition of the eluted polymer.

Investigation and modeling of the phase compositions and densities during the hydrogenation of carbon dioxide to methanol under supercritical conditions

K. Vogel, H. Vogel, Technische Universität Darmstadt, Ernst-Berl-Institute of Technical Chemistry and Macromolecular Science, D-64287 Darmstadt, Germany

Introduction

Nowadays, the use and development of renewable energy is an important subject. In Germany the production of electricity from wind and photovoltaic plants plays a major role. The main disadvantage of the energy sources is the fluctuation of sunlight and wind respectively. One way to overcome this drawback could be the chemical storage of the electrical energy. In this case the production of methanol from carbon dioxide and solar-hydrogen, which is produced via electrolysis of water, offers a high potential. Methanol has the advantage that the energy can be retrieved when it is needed and in addition it can be easily stored and transported. [1], [2]

The aim of this work is to study the phase behavior and the densities of the reaction mixtures during the methanol synthesis from carbon dioxide and hydrogen. The measurements are carried out at temperatures between 150 – 350 °C and pressures up to 16 MPa. Initially carbon monoxide is neglected. The experimental equipment described below are currently under construction and might need to be extended or adapted.

Experimental

Phase determination

A cylindrical high pressure view cell is used for the determination of the phase behavior. The cell is composed of Inconel 625 and has a volume of 5 cm^3. Through two opposing graphite sealed sapphire windows, the whole content can be visually observed and recorded by a webcam (Logitech, C920). A magnetic bar is used for stirring the fluid. Liquid components (methanol, water) can be injected by a screw press (HIP/PTG Pressure Technology GmbH, 62-6-10). A pump (Knauer GmbH) is used to feed liquefied CO_2 (Westfalen AG, 3.8). A high pressure mass flow controller (Bronkhorst) is used to feed H_2 from a 30 MPa gas cylinder (Linde AG, 5.0). The cell is heated with cartridge heaters (4 x 500 W) and the temperature is determined with a thermocouple (type K) located in the fluid.
For an experiment the cell is initially pressurized with hydrogen and expanded. This process is repeated at least five times. After that the multicomponent mixture is

placed in the cell. The addition of the substances is carried out successively in the order: H_2, CO_2, liquid components. The amounts of water and methanol are calculated by the added volume, the amount of CO_2 is calculated by the flow rate and time and the amount of H_2 is calculated by the initial pressure. To verify the calculated quantities of CO_2 and H_2, further experiments are performed in which the additions takes place via pressure vessels and the amounts of substance are calculated from the mass differences. The phase transitions are determined as a function of pressure, temperature and composition.

Determination of density

An oscillating U-tube apparatus (Anton Paar, DMA HDT) is used for the density measurements. The measuring cell consists of the measuring transducer, the sensor and field coil, a thermostat and two thermocouples (Pt100). Control and data acquisition is carried out via a DMA control computer. In front of the measuring cell is a preheating, which minimizes the temperature gradient between the measuring cell and the inlet.
The mixture to be tested is continuously passed through the apparatus at the experimental conditions (pressure, temperature). A high pressure mass flow controller (Bronkhorst) is used to feed H_2 from a 30 MPa gas cylinder (Linde AG, 5.0). A pump (Knauer GmbH) is used to feed liquefied CO_2 (Westfalen AG, 3.8). Another pump (Hitachi) is used to feed methanol / water mixtures. The system pressure is set by an overflow valve. After calibration with pure H_2 and pure CO_2 the density is determined as a function of pressure, temperature and composition.

Expectations

From the phase tests, the number of phases, during the methanol synthesis can be obtained. For the single-phase region, the densities as a function of pressure, temperature and composition can be determined using the apparatus describe previously. In the next step the experimental data are attempted to model with cubic equations of state in combination with mixing rules.

References

[1] G. Olah, A. Goeppert, G. Prakash, *Beyond Oil and Gas: The Methanol Economy*, 1st ed., Wiley-VCH, Weinheim, **2006**.
[2] S. Jadhav, P. Vaidya, B. Bhanage, J. Joshi, *Chem. Eng. Res. Des.*, **2014**, *92*, 2557-2567.

Corrosion and Liner Technology in Ammonothermal Synthesis

Anna-C. L. Kimmel, Friedrich-Alexander-Universität Erlangen-Nürnberg

Ammonothermal synthesis

Ammonothermal synthesis is a promising solvothermal crystal growth process, which allows the growth of many different compounds: inter alia imides, ammoniates and group III nitride single crystals [1]. The most popular example is gallium nitride (GaN), an innovative semiconductor for the energy efficient generation of blue light in light emitting diodes (LEDs).

Figure 1 shows a typical autoclave setup with two temperature zones used for ammonothermal crystal growth. A mixture of supercritical ammonia with solubility increasing additives (mineralizers) dissolves precursor material (e.g. polycrystalline GaN) and forms metastable complexes, so called intermediates. This takes place in the saturation zone of the autoclave (T_2). Due to the temperature change in the growth zone ($T_1 < T_2$, if the temperature coefficient of solubility is positive) the diluted precursor recrystallizes on provided seed crystals (e. g. monocrystalline GaN).

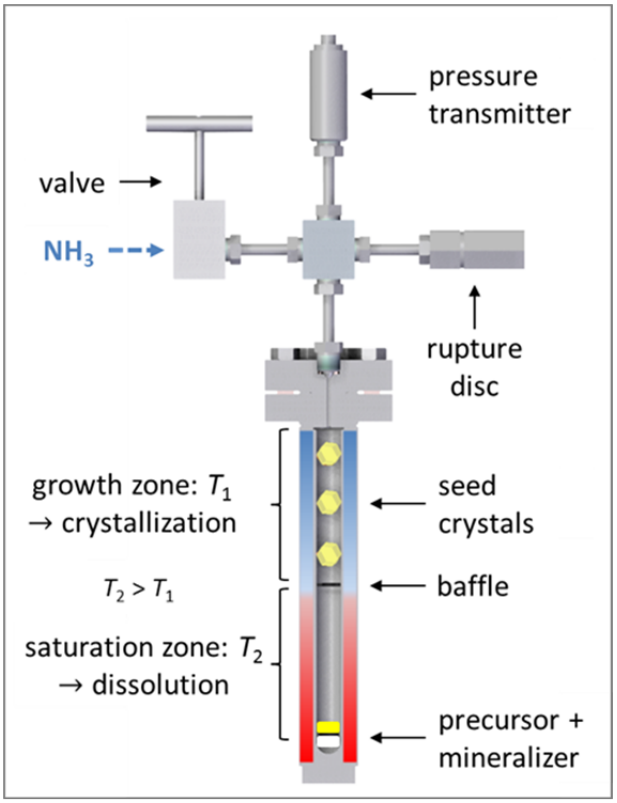

Figure 1: Autoclave setup for ammonothermal crystal growth with positive temperature coefficient of solubility.

Transport from the saturation zone to the growth zone is realized by means of convection – the temperature gradient between the two zones of the autoclave is typical between 20 and 50 °C [2].

Depending on the provided mineralizer, two main routes of ammonothermal synthesis can be distinguished: the ammonobasic or ammonoacidic route with alkali metal amides or ammonium halides as mineralizers respectively. Depending on the mineralizer the chemistry of the solution changes significantly and leads to different process conditions, crystal qualities and corrosion behavior.

Process conditions are very harsh in ammonothermal synthesis: temperatures of 400 - 800 °C and pressures up to 300 MPa are applied. Additionally, autoclave and process equipment are exposed to the highly reactive ammonothermal medium over a long time: from a few hours to several days or weeks per run. Corrosion due to dissolution of autoclave material results in dislocations in grown crystals and may lead to failure of experimental equipment. Therefore the autoclave material has to exhibit high temperature strength besides excellent corrosion resistance. The aim of our research is to investigate, test and apply new autoclave materials and liner technologies to reach higher synthesis temperatures and reduce influence of corrosion products on grown crystals. Thus the crystal quality should be increased significantly.

Corrosion of autoclave material under ammonothermal conditions

Nickel based alloys show good high-temperature strength up to 600 °C, such as Inconel© alloy 718 (2.4668) with a yield strength of approximately 1000 MPa). That is why we use this alloy as autoclave material. In spite of general high corrosion resistance of nickel based alloys, they show limited corrosion resistance under ammonothermal conditions.
We/Hertweck et al. recently published the different corrosion behavior of alloy 718 in ammonoacidic and ammonobasic environment [3, 4]. Figure 2 shows SEM pictures of the inner autoclave surface before (a) and after approximately 50 ammonoacidic (b) and ammonobasic (c) experiments. The use of basic mineralizer leads to nitriding of the inner autoclave wall. This nitrified corrosion layer degenerates gradually due to cyclic thermal spalling. Experiments with acidic mineralizers result in much more severe corrosion, even stress corrosion cracking is observable.

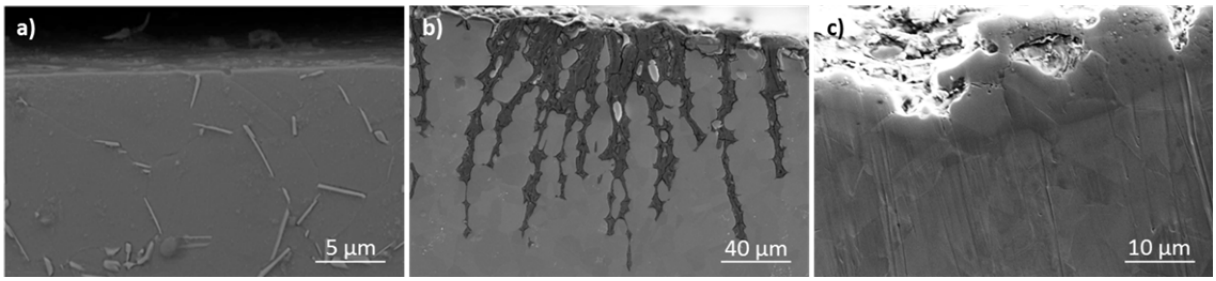

Figure 2: SEM pictures of a) surface of new alloy 718 autoclave after honing, b) inner autoclave wall after approx. 50 ammonoacidic loads, c) inner autoclave wall after approx. 50 ammonobasic loads [3].

New nickel and cobalt based alloys as alternative autoclave materials

Higher growth temperatures gain more and more scientific interest, to increase crystal quality [2]. Synthesis temperatures up to 600 °C and maximum pressure of 300 MPa can be carried out in the described Inconel-718 autoclaves. However, this alloy loses its strength above 600 °C due to changes in the microstructure of the alloy.
To reach elevated temperatures up to 800 °C other alloys with higher temperature strength are needed, e.g. Rene 41 alloy or alloy 282. Figure 3 shows the maximum internal pressure of alloy 718 and alloy 282. Yield strength of alloy 718 stays stable at about 1000 MPa up to 600 °C, resulting in a maximum internal pressure of about 300 MPa at 650 °C. In comparison the yield strength of alloy 282 stays stable up to 850 °C,

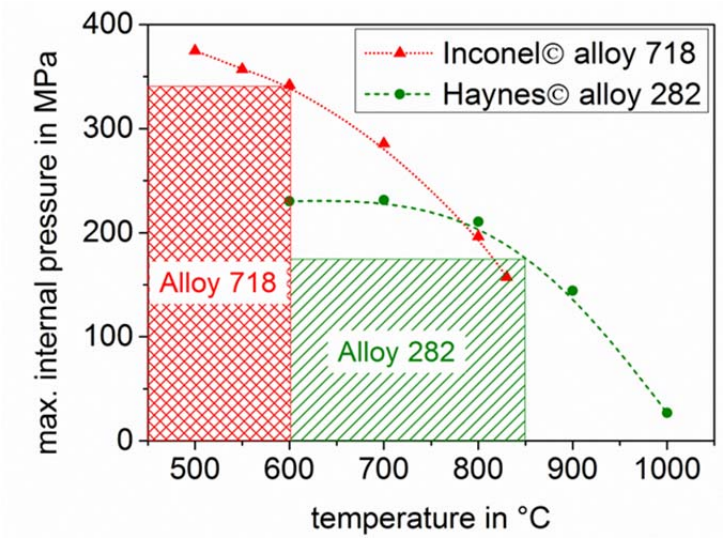

Figure 3: maximum internal pressure in Inconel© alloy 718 and Haynes© alloy 282 autoclaves depending on temperature

though with lower value of about 530 MPa. The resulting maximum internal pressure of alloy 282 is 170 MPa.
Similar to alloy 282 cobalt based alloys promise higher temperature stability than alloy 718 besides good machinability [5]. Currently we investigate the different corrosion behavior of alloy 718, alloy 282 and two newly developed cobalt based alloys in two different ammonoacidic environments. The used mineralizers are ammonium chloride (NH_4Cl) and ammonium fluoride (NH_4F). Preliminary experiments indicate that Alloy 718 shows higher corrosion rates than alloy 282 in NH_4F containing supercritical ammonia. By use of an NH_4Cl mineralizer alloy 718 seems to have higher resistance than alloy 282 in long term experiments. Besides, exposure time might have a big influence on the corrosion rate as well, therefore the time dependence is going to be investigated next.

Strategies to prevent corrosion

As corrosive degeneration occurs for all tested autoclave alloys in ammonothermal environment, liner technologies are indispensable to reduce the influence of diluted autoclave material on the crystal quality. Until recently platinum crucibles were typically used in ammonoacidic synthesis. In newer research also silver liner systems are applied [6]. In recently published experiments different ceramic coatings showed poor stability either physical (thermal spalling) or chemical (low corrosion resistance) [7]. Silicon nitride and polycrystalline silicon carbide can be used as crucible material, if the pressure in and outside of the crucible is balanced [7].
Hertweck et al. investigated the applicability of noble metal coatings as corrosion protection in ammonoacidic crystal growth [8]. Similar to corrosion resistance of the described nickel and cobalt based alloys, the corrosion behavior of the noble metal coatings strongly depends on the used mineralizer. Platinum, which showed good resistance in NH_4Cl containing ammonothermal solution, was implemented in a three layer coating. An alloy 718/Au/Pd/Pt-coating was chosen to reduce the differences in thermal expansion. This system possessed good resistance in presence of NH_4Cl, but poor resistance in presence of NH_4F. High durability in an NH_4F containing ammonothermal medium showed an alloy 718/Au/Ag two layer coating. Mechanical stability and long term behavior of the coatings still need to be tested. The next step is to implement a coated autoclave for corrosion and growth experiments to verify its assumed benefits. Furthermore the contact corrosion of precursor material on the coating and autoclave material will be investigated.

References

1. Richter, T. and R. Niewa, *Chemistry of Ammonothermal Synthesis.* Inorganics, 2014. **2**(1): p. 29-78.
2. Yoshida, K., K. Aoki, and T. Fukuda, *High-temperature acidic ammonothermal method for GaN crystal growth.* Journal of Crystal Growth, 2014. **393**: p. 93-97.
3. Hertweck, B., et al., *Different corrosion behaviour of autoclaves made of nickel base alloy 718 in ammonobasic and ammonoacidic environments.* The Journal of Supercritical Fluids, 2014. **95**(0): p. 158-166.
4. Hertweck, B., et al., *Corrosive Degeneration of Autoclaves for the Ammonothermal Synthesis: Experimental Approach and First Results.* Chemical Engineering & Technology, 2014. **37**(11): p. 1903-1906.

5. Suzuki, A., G.C. DeNolf, and T.M. Pollock, *Flow stress anomalies in γ/γ' two-phase Co–Al–W-base alloys.* Scripta Materialia, 2007. **56**(5): p. 385-388.
6. Pimputkar, S., et al., *Improved growth rates and purity of basic ammonothermal GaN.* Journal of Crystal Growth, 2014. **403**: p. 7-17.
7. Hertweck, B., et al., *Ceramic liner technology for ammonoacidic synthesis.* The Journal of Supercritical Fluids, 2015. **99**(0): p. 76-87.
8. Hertweck, B., et al., *Applicability of Metals as Liner Materials for Ammonoacidic Crystal Growth.* Chemical Engineering & Technology, 2014. **37**(11): p. 1835-1844.

Study on the effects of electric currents passing through roller bearings causing bearing failures

Manuel Zuercher, Friedrich-Alexander-Universität Erlangen-Nürnberg

Bearings and Lubrication

One of the most important machine components are bearings. These elements are used in every kind of moving engine, i.e. cars, electric motors or wind turbines. Their main task is to reduce friction which is created on the moving parts. To support this reduction lubricants are added to achieve even lower friction, minimize abrasion and to dissipate heat. These fluids can be gaseous, liquid or even solid like. Nevertheless, mostly liquid lubricants like poly alpha are used. These oils are generally divided in synthetic and mineral oils. Synthetic oils are the reactions product of chemical synthesis from smaller hydrocarbons. These oils have a defined chemical structure and are mostly used for special applications because of their higher costs. Much cheaper are mineral oils, these lubricants, which arte more often applied, are the product of crude oil productions. The chemical composition often is not completely known and consequently the behavior in the rolling contact is difficult to predict which sometimes can lead to bearing failures. [1, 2]
To improve the physical properties of liquid lubricants and avoid early failure so called additives are added to the fluid. These additives can among other things improve the viscosity-temperature behavior, act as antioxidants, cause minor friction, prevent corrosion or care for a more stable lubricant film. Most of them are added in a liquid or solid state. Newer research even showed that gaseous additives like CO_2 can be added to improve the viscosity temperature behavior. But in general mostly lubricant dissolvable salts are applied. [1, 3]

Bearings under the influence of electric currents

Electric currents passing through bearings can be found in a lot of technical applications where electricity is either consumed or generated. Important examples are electric motors and turbines. In this context bearing failures are reported mostly due to high currents. The damage pattern which can be found in the running surface is fluting and pitting in consequence of punctual surface fusing. This effect can be attributed to discharges through the lubrication film, Which are the result of electric potentials that accrue on the rolling surfaces due to magnetic asymmetries in the machines, unwanted shaft voltages or external applied voltages. Also naturel inductive currents or brushing turbine blades can cause an electric charging of bearings. A roller bearing resembles two plate capacitors each parallel-connected to a resistor. The lubricant acts as the dielectric material between the plates. If the applied voltage exceeds the breakdown voltage the lubricant loses its isolating character resulting in an electric discharge. The breakdown voltage on the one hand depends on the physical parameters of the lubricant which are viscosity, density, chemical structures and added additives. On the other hand the type of bearing, the bearing speed and the applied axial or radial forces have a high influence, too. For example by increasing the bearing speed the lubrication film thickness increases by which means the isolation through the lubricant should increase as well.

To visualize and monitor the discharges in industrial applications as well as in most experimental setups an oscilloscope is connected parallel to the bearing. Based on the applied current the effect on the bearing surfaces can be negligible or lead to harsh damages. In literature the critical current density is 0,1 A/mm^2, if the current is below no fluting or pitting was found as a result of discharges. [4]

The bearing test rig

For the study of the electric currents passing through roller bearings a test bench has been build which is shown in figure 1 as a simplified flow chart, a picture is shown in figure 2.

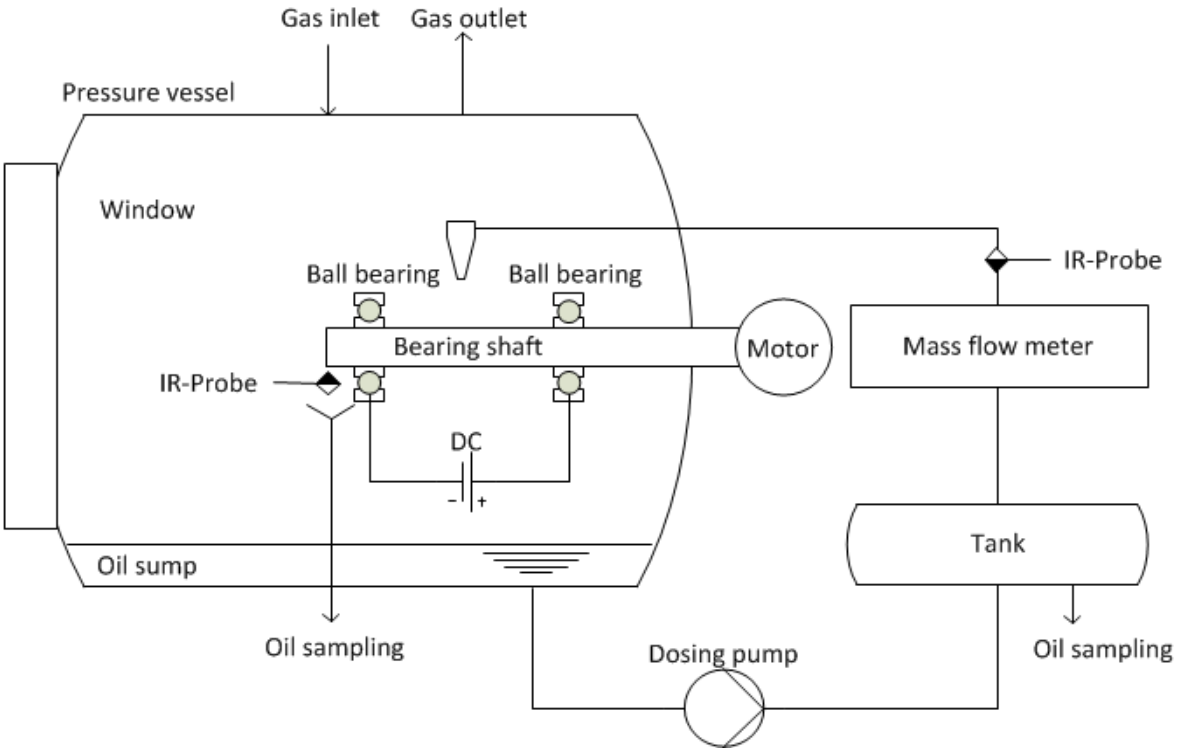

Figure 1: Simplified flow chart of the bearing test rig

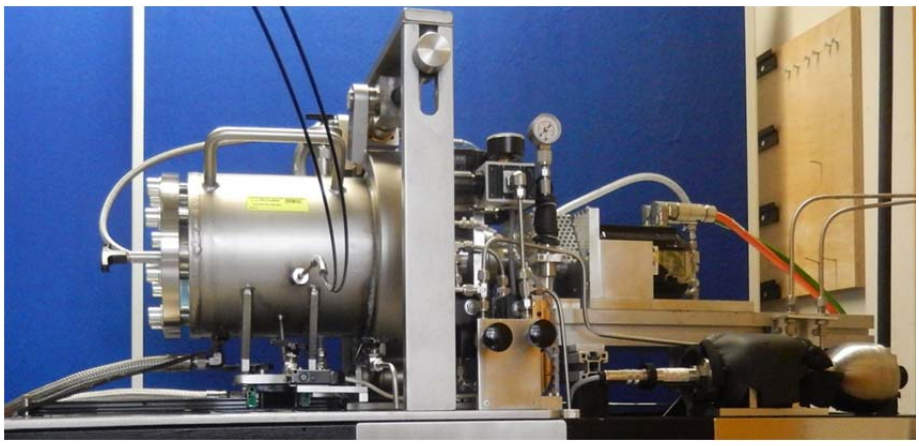

Figure 2: Picture of the bearing test rig

To avoid external influences two common roller bearings 6203-C C3 generation C (FAG) are placed on a shaft which is inside a pressure vessel with a window for

optical surveillance. The speed can be varied between 100 rpm and 5500 rpm and is powered by an electric motor. The oil is aspirated from the oil sump into the circulating fluid system by a dosing pump. The oil volume flow can be changed between 0,1 ml/min up to 144 ml/min. To exactly measure this flowrate a mass flow meter is placed beyond a tank where the oil can be sampled and heated up to 100°C. To ensure a constant and defined bearing temperature the bearing can be heated as well up to 100°C and are individually monitored. For the lubrication a semi-synthetic transmission oil is used. To lubricate the bearings the oil is supplied from above and distributed to both bearings equally. The oil which flows through the front bearing can be chemical analyzed in two ways: directly in the test rig with an infrared probe or samples of the oil can be analized in a laboratory. This optical ATR-IR-probe (infrared fiber sensors, Aachen) is connected to a Nicolet 6700 FT-IR spectrometer (ThermScientific). Thus it is possible to get a direct IR-spectrum with a sampling rate of one spectrum every 30 seconds. By doing so the chemical changes within the oil resulting from the electric currents can be detected.
The additional electrical load is applied to the bearing by connecting a DC power supply to the cups. The circuit diagram is presented in Figure 3.

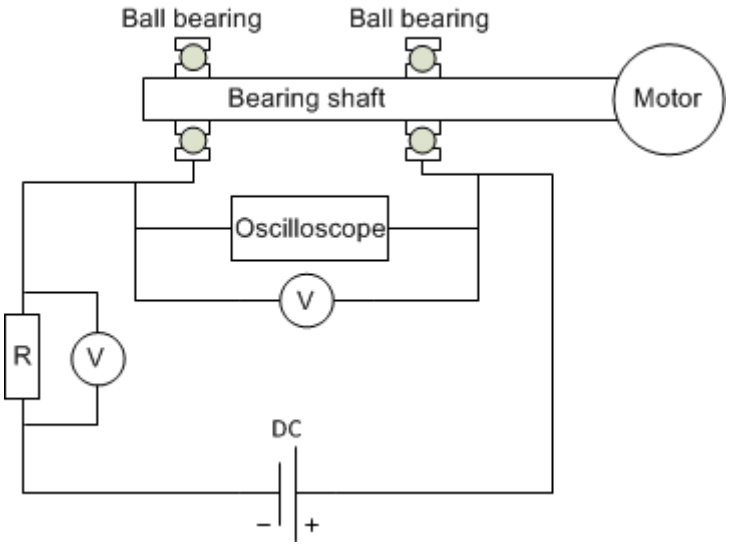

Figure 3: Circuit diagram

The electric circuit is closed through the shaft, resulting in one cup being the positive pole and one being the negative pole. Parallel to the bearing shaft an oscilloscope and a voltmeter are placed to measure and observe the discharges. To control the current a resistor is connected in series and monitored by an additional voltmeter. During the experiments a 520 kOhm and a 320 kOhm resistor will be used by which means the current density is always appreciably below 0,1 A/mm^2. In this way no negative surface damages should occur in consequence of discharges.

The next experiments

The aim of the next experiments is to detect if and which chemical changes are happening within the lubrication gap. Within these gaps very harsh reaction conditions are present. Very high pressures and high temperatures can cause all kinds of different reactions within the oil and on the metal surfaces. At the moment

most reactions in that gap are unknown but are most likely responsible for early bearing failures especially when additional electric currents are passing through the bearings.

References

1. Mang, T. and W. Dresel, *Lubricants and lubrication*. 2., completely rev. and extended ed. ed. 2007, Weinheim: Mang, Theo.
2. Bartz, W., *Einführung in die Tribologie und Schmierungstechnik* 2010, Renningen: expert-verl. 372 S.
3. Pohrer, B., et al., *CO2 as a Viscosity Index Improver for Wind Turbine Oils.* Industrial & Engineering Chemistry Research, 2015. **54**(21): p. 5810-5819.
4. Schaeffler (4), T.A.C.K. *Stromisolierende Lager*. 2011 06.08.2014 06.08.2014]; Available from: http://www.schaeffler.com/remotemedien/media/_shared_media/08_media_library/01_publications/schaeffler_2/tpi/downloads_8/tpi_206_de_de.pdf.

Scale-up of a High-Pressure Flow-Through Fixed-Bed Reactor for an Integrated Biorefinery Concept

Hannah Singer, Institute of Thermal Separation Processes, Hamburg University of Technology, Eissendorfer Str.38,D-21073 Hamburg, Germany

Concepts of integrated biorefineries using second generation substrates, such as lignocellulose, focus on the sustainable production of energy and valuable bio-based chemicals. Thereby, an economic operation mode of so far established and prospectively planned industrial plants constitutes a considerable challenge. In this regard, it is necessary to investigate the scalability of fortunate lignocellulose-conversion processes, previously evaluated at laboratory scale. Process modeling poses thereby a powerful and cost-effective tool to investigate and evaluate the scalability and optimize operating conditions in an economic and ecological way.

In order to convert lignocellulosic biomass into high-value products, the promising combination of liquid hot water (LHW) and enzymatic hydrolysis is investigated in a high-pressure flow-through fixed-bed reactor. This process setup promises a sustainable degradation, disclaiming organic solvents and acids as applied in conventional biorefineries. The lignocellulosic material mainly consists of cellulose, hemicellulose and lignin, whereby the focus of the BMBF funded project ‘Bioraffinerie 2021’ is the production of highly pure lignin. Lignin comprises basically a cross-linked network of phenol groups and is a promising component for an industrial application as filling material in adhesive tapes, thermoplastic polymers, absorbers and insulating material. Whereas, it is mostly generated as a byproduct and used as energy source via combustion in conventional biorefinery. Volatile organic compounds (VOC) incorporated in the lignin often exhibit a challenge to be overcome for industrial applications in consumer business, while they are of great interest as aromatics in food industry in parallel. A cascade process of LHW-pretreatment, enzymatic hydrolysis and high pressure extraction of the VOCs from the lignin network with compressed gases enable the production of a natural and low odor lignin at the TVT-TUHH.

Since the focus of the integrated biorefinery at the TVT-TUHH lies on the production of lignin all process steps were optimized to gain high lignin yields. In previous studies we evaluated efficient process conditions in a 3 L laboratory unit. Additionally, a model was successfully established to predict hydrolysate and solid biomass concentrations during LHW-hydrolysis. The model based on a first order pseudo homogenous reaction, respecting changing fixed-bed properties, non-ideal flow (axial dispersional effects) and temperature gradients in axial direction during the pretreatment step.

Further a pilot plant for LHW and enzymatic hydrolysis was successfully commissioned including solid and liquid separation via decantation and drying. Experimental results from both biomass degradation steps and scales were compared and evaluated. Constructional improvements of the biorefinery plant setup

and the fixed-bed stabilizer during plant commissioning enable both, stable process conditions and optimal product handling.

The present study aims at the pilot scale production of lignin to be applied as sustainable filling material to adhesive tapes. Therefore the scalability of both, the hydrothermal and enzymatic hydrolysis from laboratory (3 L) to pilot scale (40 L) was investigated. For this purpose, the scale-up was experimentally executed in different operation modes and the model of liquid hot water hydrolysis was adapted to pilot scale.

Results obtained by the experimental scale-up of the LHW indicate a more rapid and efficient degradation of hemicellulose by an optimized temperature control at pilot level. Additionally, it could be demonstrated that the circulation of the solvent (water) during LHW led to a saving of 60 wt% of solvent compared to discharge mode and 10 wt% compared to the solvent-to-solid ratio in circulation mode at laboratory scale. In the model-based LHW scale-up, the heat transfer coefficients and the dispersion coefficient were found to be the most influencing variable parameters on the process predictability.
Furthermore, it has been shown that the enzymatic D-glucose yields at both scales were comparable with each other and that this process performed best under ambient pressure and moderate temperature conditions at 50 °C.

Biopolymer-based aerogels for food applications

Imke Meissner, Institute of Thermal Separation Processes, Hamburg University of Technology, Eissendorfer Str.38,D-21073 Hamburg, Germany

1. Aerogels – properties and applications

Aerogels are highly porous solid materials with low density, high and interconnected porosity, large specific surface area, pores sized from micro to macro pores, low thermal conductivity, and low sound velocity[1–3]. Due to these unique properties aerogels are often used as thermal insulators, sound insulators, filters, and adsorbents[4]. Also the use as drug carriers and pharmaceutical applications are investigated[5], due to promising properties like biocompatibility[6] and biodegradability[7].

2. Production of aerogels

The formation of aerogels is realized by the preparation of a polymer solution or a sol, gelling of this solution, and subsequent drying of the formed gel.

2.1 Polymers

The first and most common components for the formation of aerogels have been inorganic components like silica. Kistler et al. prepared the first aerogels from inorganic and organic components in 1931[3,8]. Inorganic matrices are widely used for the production of aerogels for different applications. Many biopolymers (especially polysaccharides and proteins) are recently investigated for the production of aerogels[5,9,10]. The use of biopolymers for the production of aerogels is motivated by the abundancy of many biopolymers and often by their price advantage over synthetic polymers. Further the biopolymers are biocompatible and biodegradable[6], non-toxic, easily handled, stable, and renewable[7,11] what make them necessary and suitable for the use in medical applications and food industry.

2.2 Biopolymer-based hydrogel

The gelling of the polymeric solution leads to hydrogels, which have (mostly) water as solvent within the gel structure. The gelling can be achieved by different mechanisms depending on the chosen biopolymer, additives, and the environmental conditions. Gelation methods are for example thermal treatment (heating and cooling of the solution), pH induced gelation (with added acids or bases), addition of cross-linking agents, ultrasonic, or high pressure CO_2 induced gelation. Especially for the application in foods and pharmaceutics no toxic chemicals must be used during the preparation and the drying of the aerogels. This limit is an additional task for the production of aerogels.

The gelation with pressurized CO_2 brings some advantages compared to atmospheric conditions or high pressure nitrous oxide[12–14]. CO_2 is already used in food industry[15] and is not harmful[16]. For few different biopolymers the high pressure

CO_2 induced gelation has been proposed in literature. The gelation of various biopolymers such as silk fibroin[12,13], alginate[1], and elastin[14,17,18] has been demonstrated in the literature. Improved textural and mechanical properties have been achieved compare to gelation at atmospheric conditions[18] or high pressure nitrous oxide[12].

2.3 Drying methods

The common drying methods for hydrogels are supercritical drying with CO_2, freeze drying, and atmospheric drying. The different drying methods lead to different types of dried gels:

- Aerogels are obtained by the drying with supercritical (mostly) CO_2
- Cryogels are obtained via freeze-drying
- Xerogels are obtained by drying at atmospheric conditions

Different methods of drying cause different properties of the dried gels. Atmospheric drying leads to strong shrinkage and a strong loss of properties[19]. Freeze-drying is suitable for the receipt of some of the hydrogel properties but leads (often) to larger pores and a lower specific surface area[9,20]. Supercritical drying seems to be the most sufficient to retain the properties of the hydrogels, nearly no shrinkage occurs and highly porous, low density materials are obtained[21]. However, a solvent exchange is necessary before the supercritical drying. Thanks to the supercritical drying, aerogel structure remains almost unchanged compare to the parent wet gel. Therefore aerogels can be described as gels which hold air within the structure[3,4].

Thus, supercritical drying is the only way to produce highly porous materials out of the wet gels. As stated above, this method can be applied to inorganic and organic including biopolymer gels. The later ones are of keen interest in food application as they are biodegradable, biocompatible[22], have high porosity and specific surface area, and low densities[23]. Another advantage of biopolymer aerogels is that they possess improved mechanical properties compare to silica aerogels[3]. Biopolymer aerogels are also reported to be suitable for medical applications[12,13].

3. Research topic

The gelation of aqueous biopolymer solutions under high pressure CO_2 will be investigated. Therefore it is necessary to have the apparatus to apply high pressure CO_2 to the biopolymer solution at constant temperatures. A high pressure viewing cell will allow to observe the gelation of the biopolymer solution and a sufficient monitoring of the process parameters to investigate the gelation behavior and the properties of obtained hydrogels and aerogels.

Biopolymers with promising properties will be chosen for further investigations. Biopolymer-based aerogels should be used for the application in foods. Therefore it is also necessary to avoid the use of toxic chemicals entirely, even for additives or cross-linking agents. A lot of applications are possible for aerogels in foods.

Therefore, different properties should be reached, like high surface areas, high porosity, hydrophobicity or hydrophilicity, or large pores depending on the required application. Appropriate materials have to be chosen to reach the required properties. Therefore hybrid biopolymer-based aerogels will be investigated. The properties of the obtained aerogels can be influenced by the choice of the biopolymers (pure or mixed), the conditions of the gelation, the drying method, and additives or cross-linking agents.

References

1. Gurikov, P., Raman, S. P., Weinrich, D., Fricke, M. & Smirnova, I. A novel approach to alginate aerogels: carbon dioxide induced gelation. *RSC Adv.* **5,** 7812–7818 (2015).

2. Litschauer, M. *et al.* Silica modified cellulosic aerogels. *Cellulose* **18,** 143–149 (2011).

3. Tan, C., Fung, B. M., Newman, J. K. & Vu, C. Organic aerogels with very high impact strength. *Adv. Mater.* **13,** 644–646 (2001).

4. Cai, J., Kimura, S., Wada, M., Kuga, S. & Zhang, L. Cellulose aerogels from aqueous alkali hydroxide-urea solution. *ChemSusChem* **1,** 149–154 (2008).

5. García-González, C. a., Alnaief, M. & Smirnova, I. Polysaccharide-based aerogels - Promising biodegradable carriers for drug delivery systems. *Carbohydr. Polym.* **86,** 1425–1438 (2011).

6. Hoepfner, S., Ratke, L. & Milow, B. Synthesis and characterisation of nanofibrillar cellulose aerogels. *Cellulose* **15,** 121–129 (2008).

7. Veronovski, A., Knez, Ž. & Novak, Z. Preparation of multi-membrane alginate aerogels used for drug delivery. *J. Supercrit. Fluids* **79,** 209–215 (2013).

8. Kistler, S. S. Coherent Expanded Aerogels and Jellies. *Nature* **127,** 741 (1931).

9. Betz, M., García-González, C. a., Subrahmanyam, R. P., Smirnova, I. & Kulozik, U. Preparation of novel whey protein-based aerogels as drug carriers for life science applications. *J. Supercrit. Fluids* **72,** 111–119 (2012).

10. Elzoghby, A. O. Gelatin-based nanoparticles as drug and gene delivery systems: Reviewing three decades of research. *J. Control. Release* **172,** 1075–1091 (2013).

11. Cai, H. *et al.* Aerogel Microspheres from Natural Cellulose Nano fi brils and Their Application as Cell Culture Sca ff old. (2014).

12. Floren, M. L., Spilimbergo, S., Motta, A. & Migliaresi, C. Carbon dioxide induced silk protein gelation for biomedical applications. *Biomacromolecules* **13,** 2060–2072 (2012).

13. Mallepally, R. R., Marin, M. a. & McHugh, M. a. CO2-assisted synthesis of silk fibroin hydrogels and aerogels. *Acta Biomater.* **10,** 4419–4424 (2014).

14. Annabi, N., Mithieux, S. M., Weiss, A. S. & Dehghani, F. Cross-linked open-pore elastic hydrogels based on tropoelastin, elastin and high pressure CO2. *Biomaterials* **31,** 1655–1665 (2010).

15. Hung, T. N. *et al.* Improvement of the water brewing of Vietnamese green tea by pretreatment with supercritical carbon dioxide. *J. Supercrit. Fluids* **62,** 73–78 (2012).

16. Fernandes-Silva, S. *et al.* Porous hydrogels from shark skin collagen crosslinked under dense carbon dioxide atmosphere. *Macromol. Biosci.* **13,** 1621–1631 (2013).

17. Annabi, N., Mithieux, S. M., Weiss, A. S. & Dehghani, F. The fabrication of elastin-based hydrogels using high pressure CO2. *Biomaterials* **30,** 1–7 (2009).

18. Annabi, N. *et al.* Synthesis of highly porous crosslinked elastin hydrogels and their interaction with fibroblasts in vitro. *Biomaterials* **30,** 4550–4557 (2009).

19. Brown, Z. K., Fryer, P. J., Norton, I. T. & Bridson, R. H. Drying of agar gels using supercritical carbon dioxide. *J. Supercrit. Fluids* **54,** 89–95 (2010).

20. Obaidat, R. M., Tashtoush, B. M., Bayan, M. F., T. Al Bustami, R. & Alnaief, M. Drying Using Supercritical Fluid Technology as a Potential Method for Preparation of Chitosan Aerogel Microparticles. *AAPS PharmSciTech* (2015). doi:10.1208/s12249-015-0312-2

21. Banerjee, S. & Bhattacharya, S. Food Gels: Gelling Process and New Applications. *Crit. Rev. Food Sci. Nutr.* **52,** 334–346 (2012).

22. García-González, C. a., Carenza, E., Zeng, M., Smirnova, I. & Roig, A. Design of biocompatible magnetic pectin aerogel monoliths and microspheres. *RSC Adv.* **2,** 9816 (2012).

23. Kobayashi, Y., Saito, T. & Isogai, A. Aerogels with 3D Ordered Nanofiber Skeletons of Liquid-Crystalline Nanocellulose Derivatives as Tough and Transparent Insulators. *Angew. Chem. Int. Ed. Engl.* **126,** 10562–10565 (2014).

Process development for supercritically dried aerogels

F.Mißfeldt, Institute of Thermal Separation Processes, Hamburg University of Technology, Eissendorfer Str.38,D-21073 Hamburg, Germany

Characteristics and applications

Aerogels are nanoporous materials with unique characteristics, which were developed in the 1930's by Kistler [1]. They are highly porous solids with an open pore structure and stand out due to their high pore volume and high specific surface area. They also possess the lowest thermal conductivity, sound velocity, dielectric constant and refractive index of any solid ever measured [2]. These properties offer a wide field of different applications, for instance in Cherenkov detectors, in solar energy collector, in pharmaceutical applications as drug carriers, in waste treatment and in acoustic and thermal insulation.

Reaction mechanism

Aerogels can consist of different inorganic or organic materials, e.g. silica or starch and have in common that they are produced via a sol-gel process. The first and nowadays most widespread kind of aerogels in applications is silica aerogels. Silica aerogels can be produced from tetraethylorthosilicate (TEOS). But also other precursors like water glass or other tetraalkyl orthosilicates (e.g. TMOS) are possible. The reaction mechanism of the gel formation is hydrolysis with a subsequent condensation reaction. Both reaction steps, hydrolysis and condensation reaction, can be catalyzed either by an acid or a base. In a first step TEOS is partially hydrolyzed leading to triethylsilanol, diethylsilanediol or ethylsilanetriol or is completely hydrolyzed leading to orthosilicic acid. In a second step, the condensation reaction, the hydroxyl groups of two hydrolyzed TEOS molecules react and form a siloxane bond with expulsion of water. Further dimers and oligomers are formed and interconnected by this mechanism resulting in a gel. Then the gel is aged and subsequently dried.

Drying

Drying can be performed at ambient pressure (resulting in xerogels) or under supercritical conditions (giving aerogels). In ambient pressure drying shrinkage and collapse of the pores occur due to the high capillary pressures, which may reach 100-200 MPa [3]. Plenty of research has been done to overcome these problems for silica aerogels. To prevent shrinkage and pore collapse in ambient pressure drying, preliminary modification of the gel surface is necessary. Solvent exchange and treatment of the internal surface groups by an IPA/TMCS/n-hexane solution [4] or ETOH/TMCS/heptane solution [5] followed by ambient pressure drying lead to a 'sprinback' effect, i.e. to the restauration of the original gel volume up to 94%. However this route of surface modification is not suitable for all applications. For example the hydrophobization of the aerogel surface to achieve the 'springback' effect may lead to a reduction of the adsorption capacity in pharmaceutical applications [6].

These problems can be addressed by supercritical drying. In supercritical drying the phase transition between the liquid and vapour phase is avoided. The high capillary pressure and thus shrinkage during the supercritical drying can be avoided, so no surface modification is necessary. Therefore aerogels with any desired surface groups can be produced by supercritical drying. The latter can be distinguished between high temperature supercritical drying (HTSCD) and low temperature supercritical drying (LTSCD). In HTSCD a solvent, e.g. ethanol is brought from the liquid state into supercritical state and afterwards from the supercritical state into the vapour state to avoid the phase transition between the liquid and vapor phase. In LTSCD supercritical CO_2 is used to extract the solvent from the gel. The drying with supercritical CO_2 is favorable because of the low possible temperature ($T_{cr,CO2}$ = 30.98 °C) which may be important for loaded gels with thermally sensitive pharmaceuticals and because of the reduction of gelation time under supercritical CO_2 [7].

In this recently started work an integrated process for the aerogel production with supercritical drying shall be developed. Not only the influence of supercritical CO_2 on the gelation and the resulting aerogel properties will be further investigated but also the influence of process parameters like temperature and pressure on shape and characteristics, e.g. thermal conductivity, specific surface, density, pore volume and pore size distribution of monolithic aerogels and aerogel particles will be examined and possible process designs will be evaluated.

References

[1] S.S. Kistler, Coherent Expanded Aerogels and Jellies, Nature 127 (1931) 741.
[2] J. Fricke, T. Tillotson, Aerogels: production, characterization, and applications, Thin Solid Films 297 (1997) 212–223.
[3] P.R. Aravind, P. Shajesh, G.D. Soraru, K.G.K. Warrier, Ambient pressure drying: a successful approach for the preparation of silica and silica based mixed oxide aerogels, J Sol-Gel Sci Technol 54 (2010) 105–117.
[4] S.-W. Hwang, H.-H. Jung, S.-H. Hyun, Y.-S. Ahn, Effective preparation of crack-free silica aerogels via ambient drying, J Sol-Gel Sci Technol 41 (2007) 139–146.
[5] F. Shi, L. Wang, J. Liu, Synthesis and characterization of silica aerogels by a novel fast ambient pressure drying process, Materials Letters 60 (2006) 3718–3722.
[6] Z. Ulker, C. Erkey, An emerging platform for drug delivery: Aerogel based systems, Journal of Controlled Release 177 (2014) 51–63.
[7] I. Smirnova, W. Arlt, Synthesis of Silica Aerogels: Influence of the Supercritical CO2 on the Sol-Gel Process, Journal of Sol-Gel Science and Technology 28 (2003) 175–184.

Encapsulation of octafluorocyclobutane into lipid-based microparticles by Particles from Gas Satured Solutions (PGSS)

D. Deodato Lopes [1,2],S. Rodríguez-Rojo[3], H. Matias [1], I. Nogueira [4], C. M.M. Duarte[1,2]
[1]*Instituto de Tecnologia Química e Biológica, Universidade Nova de Lisboa, Av. República, 2780-157 Oeiras, Portugal*
[2]*Instituto de Biologia Experimental e Tecnológica, Apartado 12, 2781-901 Oeiras, Portugal,*
[3] *High Pressure Processes Group, Universidad de Valladolid, Dr Mergelina s/n-47005 Valladolid, Spain*
[4]*Universidade Técnica de Lisboa, IST, Instituto de Ciências e Engenharia de Materiais e Superfícies, P-1096 Lisboa, Portugal*

1. Introduction

Microbubbles (MBs) are spherical voids or cavities composed by a filling gas, namely a perfluorcarbon (PFC), and a coating material. MBs are used as contrast agent in U.S. imaging for disease diagnosis. Besides, MBs can be used as target drug delivery devices, having a drug incorporated in the MB and the targeting ligands coupled to the coating material [1-3]. Moreover, MBs are being studied for ultrasound triggered drug delivery. After intravenous injection, MBs as U.S. imaging contrast agents, freely circulate throughout the vasculature under low pressure pulses. When MBs reach the target organ, stronger ultrasound pulses are applied to destroy them. The drug is, thus, release and easier absorbed by cells [4]. The ligands incorporated onto the surface of MBs, enable targeting to cell-specific receptors for more precise therapy with U.S [1]. Furthermore the microbubbles in combination with ultrasounds may increase transiently the permeability of various biological barriers, such as blood-brain-barrier [4].
Gases commonly used in the synthesis of MBs are low molecular weight PFC: octofluoropropano (C_3F_8), octofluorocyclobutane (C_4F_8) and decafluorobutane (C_4F_{10}). Besides, some liquid fluoroalkanes are also used: dodecafluoropentane (C_5F_{12}), which became gas above 29.5ºC at atmospheric pressure, and tetradecafluorohexane (C_6F_{14}) [1,5].
Conventional processes for the production of MBs involved involve several steps with low gas encapsulation efficiency. Firstly, microparticles are produced and, afterwards, the gas is introduced inside the particles [5]. Recently, one step processes typically used for the production of core-shell microparticles, have been tested for the production of MBs with different success: co-axial electrohydrodynamic atomization and microfluidic devices [6].
However, the use of Supercritical Fluid (SCF) based process technology remains almost unexplored, despite of the wide application in particle formation and encapsulation processes [7].
In a previous work [9], it was demonstrated the possibility to encapsulate C_3F_8 and C_4F_8 into carrier particles (Gelucire 50/13) by PGSS (Particles from Gas Saturated Solutions). The PGSS technique, patented by Weidner and co-workers in 1995, is an attractive and simple micronization process that eliminates the need of organic solvents; it consists on the expansion of the molten carrier saturated with SC-CO_2 at relatively low pressure and temperature [8]. This process is especially suitable for the production of lipid particles and it is suitable to encapsulate liquids into lipids or plastizable polymers [7].
Best results of MBs formation by PGSS were achieved for C_4F_8 processed at 8.5 MPa and 353.15 K with a mass ratio carrier: PFC of (30:1). However the stability of the gas inside the microparticles was below 3h.
In this work, experimental conditions in the PGSS process in the two phase area of the C_4F_8-CO_2 system are being explored in order to increase the gas encapsulation efficiency. In these experiments sc-CO_2, was not used. The objective is to have a three phase system in the PGSS vessel before expansion: molten carrier, a liquid phase rich in perfluorcarbon and a gas or supercritical phase rich in CO_2. Besides, a surfactant has been added to improve the mixture between the lipid and the perfluorcarbon rich phase. For that purpose, the phase behavior between CO_2 and C_4F_8 at given mole fractions was previously checked.

2. Materials and Methods

Gelucire ® 50/13 (Hydrogenated Palm Oil PEG-32 Esters, HLB = 13; MW: 1428 g/mol), used as lipid carrier, was kindly supplied by Gattefossé (France). Tween 80 (HLB = 14.9) from Sigma-Aldrich was used as surfactant. CO_2 with 99.95% and 99,998 purity C_4F_8 (R-C318) was delivered by Praxair S.A. (Spain).
A high pressure visual cell was used to study the behavior of the carbon dioxide in the presence of perfluorobutane and the carriers. The apparatus consisted of 5 cm^3-volume high pressure cell with sapphire windows.

The experiments were performed as follows: The PFC was added in the visual cell by means of a manual syringe pump, whose piston was inside an ice bath with liquid nitrogen to guarantee that the PFC was in liquid state. Afterwards, liquefied CO_2 was injected into the system using a pneumatic pump.
The apparatus used to produce the particles; it was the PGSS (Particles from Gas Satured Solutions) in batch mode. The PGSS experimental setup (FAME UNIT, Separex, France), that consists on a high-pressure stirred vessel of 50 mL where carbon dioxide is added to the mixture of lipid and PFC at the operating temperature till the operating pressure is reached. This carbon dioxide saturated solution is further expanded through a two-fluid nozzle of 250 μm in diameter. Particles are recovered into a collector of 18L. The PFC was injected with a manual high-pressure syringe pump previously refrigerated.
FE- SEM (Field Emission Scanning Microscopy) was used to observe particle size and morphology. The quantification of the gas inside the particles was detected by NMR. A sample of dry particles together with a capillary filled with a solution of trifluoroacetic acid with D_2O (1:10) was introduced in a NMR tube.

3. Results

3.1 Phase Equilibrium

Phase equilibrium of the system CO_2- C_4F_8 is not available in literature, up to the best authors' knowledge. Nevertheless, thanks to the works of Iezzi and co-workers [10] [11] that studied the phase equilibrium of liquid PFC-CO_2 of different chain length and structure (linear, cyclic and aromatic), it can be assumed that the critical pressure of the system at low temperature (i.e. 313 K) should be around 7MPa and at high temperatures (i.e. 353 K) should be below 8-8.5 MPa.
As indicated in Figure 1, to work in the two phase region operating conditions in to different regions can be explored. Region A implies to work at high temperatures and pressures below the critical point (i.e. 353 K and 7 MPa) at relative low CO_2 mol fraction, below 0.9. At lower temperatures (313 – 323 K), region B, lower pressures are required and the two phase region can be attained at quite high carbon dioxide mole fraction, up to 0.98.

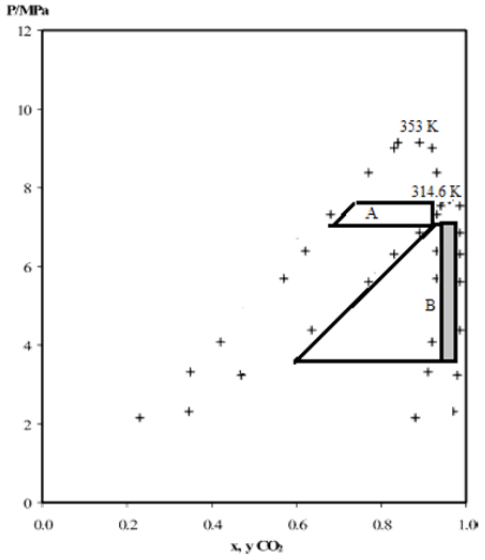

Figure 1 *Phase equilibrium of CO_2 – perfluoro-n-hexane at different temperatures measured by (Iezzi et al, 1989). Adapted from (Dias et al, 2006)*

A. 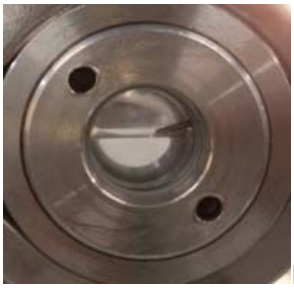 B.  C. 

Figure 2: *PFC-CO_2 at 0.98 mole fraction of CO_2 (zCO_2) and 7 MPa: A. - 313 K. B. - 323 K. - 333 K.*

Operating at high CO_2 mole fraction (shaded area of region B) is preferable from the economic point of view since perfluorocarbon gases are quite expensive.
Before carrying out the PGSS experiments, the coexistence of the two phases was verified in a high pressure visual cell. In Figure 2, it can be visualized the existence of a liquid phase in the binary system PFC-CO_2 at 0.98 mole fraction of CO_2 and 7 MPa at different temperatures. It can be seen that the interfacial surface between the gas and the liquid was almost vanished at the highest temperature tested (333K).

3.2. PGSS results
In the aim of PGSS experiments was to verify the effect of having a C_4F_8 rich liquid phase, in the amount of PFC encapsulated in the final particles and in the half life of the gas within the particles. As shown in Table 1, four experiments were performed.

Table 1. *Operating conditions of PGSS experiments*

Experiment	0 (from [9])	A	B	C	D
P (MPa)	8.5	7.2	6.1	7.0	7.0
T (K)	353	353	351	323	323
m Gelucire (g)	5.00	5.023	9.995	9.985	9.996
m Tween (g)	-	0.11	0.12	0.11	0.22
m C_4F_8 (g)	0.482	0.230	0.72	0.72	0.723
m CO_2 (g)	6.9	6.17	4.38	6.64	6.66
Z CO_2	0.985	0.992	0.965	0.977	0.977
Gel:C_4F_8 (w/w)	10	22	14	14	14

In A and B the operating pressure was decreased while keeping high operating temperature values (ca. 353 K). However, according to the value of Z_{CO2}, molar fraction of carbon dioxide at global composition of the system CO_2-C_4F_8, and the expected behaviour of the system outlined in Figure 4, there was no a liquid phase in experiments A and B. Therefore, the effect of pressure decrease in the morphology of the particles and its effect on gas retention were studied. Besides, also a surfactant (Tween 80) was used in order to improve the formation and stability of an emulsion between the gas phase of CO_2-C_4F_8 and the carrier.
As shown in Figure 2, particles produced at lower pressures (B) in comparison to experiment 0 have also sphere-like morphologic, although particle size is higher. Besides, Figure 3.B. also shows the presence of a high number of gas bubbles inside the carrier particles; this phenomenon could be due to the addition of a surfactant.
Regarding the content of C_4F_8 in the particles directly after production (Figure 4), there is a slight decrease as operating pressure is reduced.
In experiments C and D (Table 1), the effect of temperature reduction at constant pressure (7MPa) and that of the presence of a rich-PFC liquid phase is analyzed. The addition of surfactant is also analyzed. As shown in Figures 3C and 3D, the morphology of the particles obtained at lower temperatures is foam-like, particles are bigger, more porous and do not have a well defined shape. Similarly to Figure 3B, in experiment D the presence of a high number of gas bubbles inside the carrier particles was detected with the addition of surfactant. As a result of the more porous morphology, a smaller amount of gas was retained in the carrier particles at these conditions (Figure 3). The effect of the addition of surfactant was not really significant.
Besides, the fact that the expansion experimented by the liquid phase is much higher (ca. tenfold) that of the gas phase of the system CO_2-C_4F_8 at operating conditions, can also contribute to a faster release of the gas directly after production due to the burst of gas bubbles.

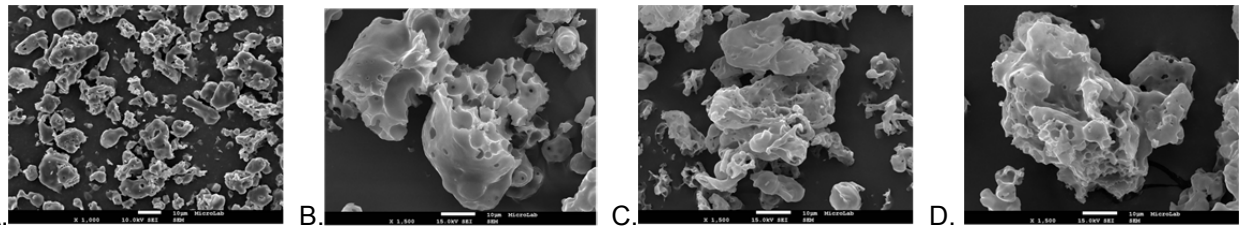

Figure 3: *SEM images (magnification X1500, Scale bar 10 μm) of particles obtained by PGSS at different operating conditions: A. experiment 0 from [9] (magnification X1000, Scale bar 10 μm). B-D. experiments according to Table 1.*

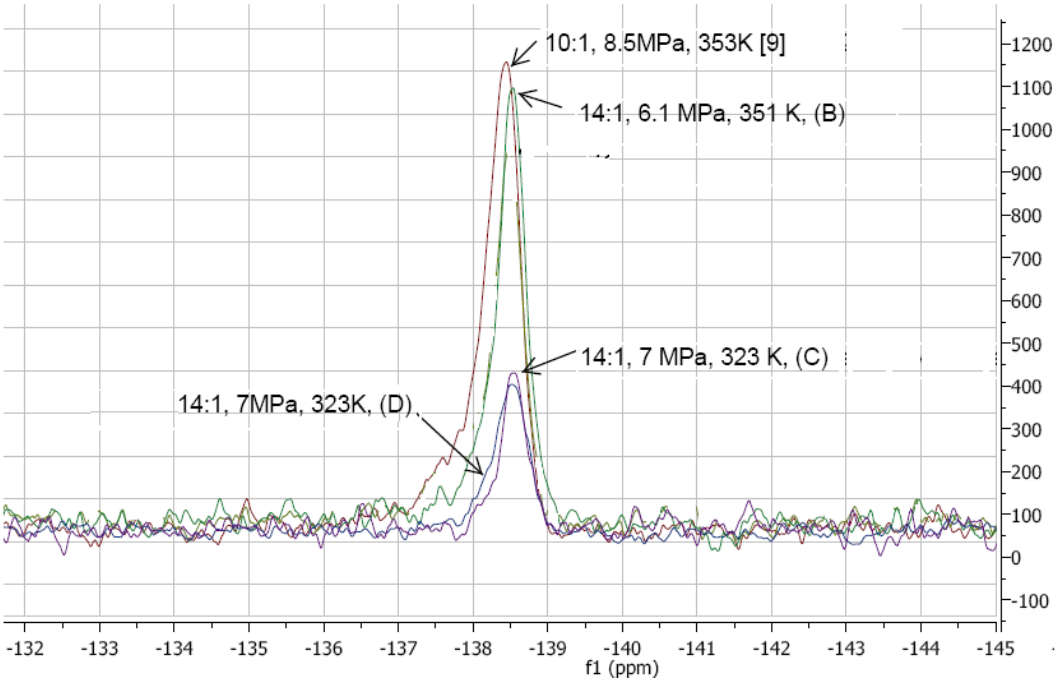

Figure 4: *^{19}F NMR spectra analysis of C_4F_8-filled Gelucire 50/13 particles produced according to the conditions specified in Table 1.*

4. Conclusion

In this work, gas-filled microparticles of Gelucire 50/13, a lipid based carrier, with C4F8 were prepared by PGSS (Particles from Gas Satured Solutions) process in batch mode. The effect of the presence or not of a liquid C_4F_8-rich phase at the operating conditions (P=6 – 8MPa, T = 313 – 353 K and CO_2 molar fractions higher than 0.95) in the high pressure vessel was studied. It was demonstrated that the use of lower temperatures and pressure produce more porous particles that retained smaller quantities of gas, according to the qualitative analysis of the fluorine atom by NMR.

The influence of the lipophilic – hydrophilic character of the carrier is also under investigation to increase the amount of encapsulated gas and its stability, however their life-time inside the particle is short, less than 3h

5. References

[1] F. Cavalieri, I. Finelli, M. Tortora, P. Mazetic, E. Chiessi, F. Polizio, B.T. Brismar, G. Paradossi. Chemistry of Materials 20 (2008) 3254-3258.
[2] E.Strider, M. Edirisinghe. Soft Matter 4 (2008) 2350-2359.
[3] E. C. Unger, T. Porter, W. Culp, R. Labell, T. Matsunaga, R. Zutshi. Advanced Drug Delivery Reviews 56 (2004) 1291– 1314
[4] K. Ferrara, R. Pollard, M. Borden. Annual Review of Biomedical Engineering 9 (2007) 415-447.
[5] S. Tinkov, R. Bekeredjian, G. Winter, C. Coester. J. Pharmaceutical Sciences 98 (2009) 1935 – 1961.
[6] K. Hettiarachchi , A.P. Lee. J. Colloid and Interface Science 344 (2010) 521–527.
[7] M.J. Cocero, A. Martín, F. Mattea, S. Varona. J. of Supercritical Fluids 47 (2009) 546-555.
[8] E. Weidner, Z. Knez, and Z. Novak, Process for preparing particles or powders, WO Patent 95/ 21688.
[9] S. Rodríguez-Rojo, D. Deodato Lopes, H. Matias, I.D. Nogueira, C.M.M. Duarte,Encapsulation of perfluorocarbon gases into lipid-based carrier by PGSS. Journal of Supercritical Fluids 82, 206-212
[10] A. Iezzi, P. Bendale, R. Enick, M. Turberg, J. Brady. Fluid Phase Equilibria 52 (1989) 307.
[11] A. M. A. Dias , H. Carrier, J. L. Daridon , J. C. Pàmies , L. F. Vega , J. A. P. Coutinho, and Isabel M. Marrucho. Industrial and Engineering Chemistry Research 45 (2006) 2341–2350.
[12] A.R. Sampaio de Sousa, Development of functional particles using supercritical fluid technology, Ph.D. Thesis, Instituto de Tecnologia Química e Biológica (Portugal), 2007.

Selective fractionation and depolymerisation of lignocellulosic biomass using subcritical and supercritical water to produce hemicellulose, cellulose and lignin.

Gianluca Gallina, High Pressure Processes Group, Department of Chemical Engineering and Environmental Technology, School of Engineering, University of Valladolid, Spain

Cellulose and hemicelluloses contained in woody biomass can be hydrolysed to monomeric sugars, which can be fermented to ethanol, or can be converted into higher value products [1].
Hemicelluloses, when isolated from biomass, have unique properties. They can be used to produce films for packaging applications in substitution to synthetic plastics, as polysaccharides works as barriers against oxygen permeation; another important application is the production of aerogels to insulate products. Xylose from hemicellulose, for instance, can be converted to furfural, which is a precursor used in different fields, such as oil refining, plastics, pharmaceutical, and agrochemical industries. L-Xylose can be also hydrogenated or enzymatically transformed to xylitol, which is a sweetening agent and is also used for preventing tooth decay [2].
The idea of transforming biomass to energy, materials, and chemicals, defines the concept of biorefinery, particularly interesting topic nowadays, considering the issues related to fossil combustibles and derivatives [3-5].
A promising, clean and cheap way to depolymerize cellulose and hemicellulose into monosaccharides is the process called autohydrolysis, which simply consists on treating biomass with hot water/steam.
During the reaction, most of the hemicellulose is extracted and hydrolysed to monomers, with a consequent release of acetic acid originated from the acetyl groups bonded to the oligosaccharides; a less amount of cellulose is released, due to the crystalline structure of the polymer, which make it more difficult to dissolve [6] .
In our study, we investigate thoroughly the autohydrolysis of wood coming from different species of trees to produce expecially hemicelluloses. The experiments are carried out with different kinds of reactors:

- a laboratory-scale semicontinuous tubular reactor , i.e. biomass wood chips in batch and fresh water pumped in continuous.
- a batch cascade reactor composed by 5 reactors connected in series, with water fully recirculated;
- a continuous reactor with a homogeneous water-sawdust slurry, injected through a pipe together with a high temperature water stream, with low residence times;
- a pilot-scale plant composed by 5 semi-continuous reactors working in series.

Fractionation of biomass from *Eucalyptus globulus*, using subcritical water with a laboratory-scale semicontinuous tubular reactor

Eucalyptus is a tree of considerable importance in the Iberian Peninsula, due to its wide expansion and its spread use in industrial applications. *Eucalyptus globulus*, in particular, is the world's most efficient tree for producing pulp. Important features are a

very high growth rate, and a high density of the wood. Another important characteristic is that, respect to other species used for biomass production, eucalyptus is one of the most efficient in water consumption. High biomass yield and low water consume make eucalyptus very attractive from an industrially point of view, not only for paper production, but also as sustainable and carbon-neutral source for liquid fuels.
The present study was performed in a semicontinuous tubular reactor, where the eucalyptus wood chips were held for all for the duration of the experiment, while a water flow was injected continuously through a HPLC pump. Different liquid flowrates (2.5, 5, 10, 15, 20 mL/min) and different reaction temperatures (135, 185, 235, 285 °C) were tested in order to determine the best conditions to extract sugars C6 and C5 from the wood. These reaction conditions allowed obtaining up to 73% of sugars from the total mass, while the degradation products were only 10%, thus minimizing the by-products. A correlation between pH and residence time was obtained in order to understand the reaction mechanism of the process.

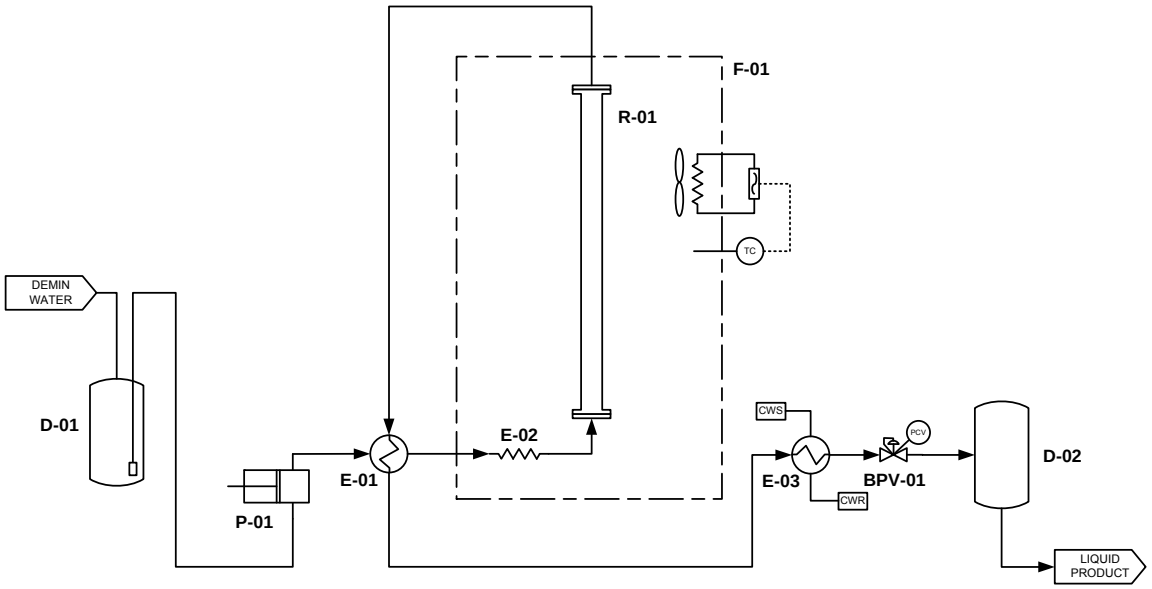

Figure 1. Schematic flow diagram of the experimental system. Equipment: D-01 Feeder, P-01 Pump, E-01 Feed water preheater, R-01 Hydrothermal reactor, F-01 Reactor air convection oven, E-02 Reactor inlet heat exchanger, BPV-01 Product depressurization Go-backpressure valve, E-03 Product cooler, D-02 liquid product vessel.

Study of hemicelluloses composition of different tree species, extraction using subcritical water with a batch cascade reactor.

Hemicelluloses from 10 different tree species commonly growing in the Castilla y Leon region have been extracted with a batch cascade reactor. Raw materials come from tree branches, cut during the seasonal pruning.

The aim is to identify the best species to obtain a high concentration of hemicelluloses, high yield and high molecular weight. The system allows the sampling of both the solid and liquid phases during the reaction. Temperature and pressure of the system are monitored and recorded online inside each reactor chamber. . Experiments were carried

out at the same operating conditions: temperature of 160°C, particle size between 1,25 and 2 mm, residence time of 80 min.
Previous works indicates these conditions to be the best to obtain the highest yield of hemicelluloses, with the lowest amount of degradation products [7].
Samples of extracted liquid solution and extracted solid were taken at 5, 10, 20, 40 and 80 min from the beginning of the experiments.
Highest amount of hemicelluloses is contained in trees of genera *Prunus*, highest yield (89%) have been reached from *Acer saccharium* (sugar maple).

Figure 2. Picture of the cascade reactor setup.

Fractionation of woody sawdust using a continuous reactor.
Sawdust produced from carpentry have been collected and sieved in order to obtain powder with a particle size lowers than 200 □m. A homogeneous sawdust-water slurry with a concentration 2%, constantly mixed was continuously injected through a pipe, and mixed with a hot water stream. The temperature of the water stream and the length of the pipe have been changed in order to maximize the yield of hemicelluloses, without breaking the cellulose chains. Temperatures between 250 and 300 °C have been chosen, with residence times between 0,8 and 5,5 seconds. The severity factor varies between 2,7 and 4,8. After the extraction, the exhaust solid was filtered from the water solution and passed through the reactor together with a supercritical water stream (400°C and 250 bar) in order to hydrolize the cellulose and obtain an exhaust solid rich in lignin. This process allows to selectively separating the three principal biomass components [8].

Pilot-scale multistage semi-continuous reactor for the extraction of hemicelluloses

The aim is to design and build a pilot plant for the extraction of hemicelluloses, composed by 5 semi-continuous reactors working in series. Each reactor has a volume of 1L and can be charged with wood particles bigger than 1 mm.
Liquid samples can be continuously collected at the outlet of every stage, in order to monitories continuously the composition of the water-sugars solution; solid samples can be taken at the end of the experiments, from different points of the bed, allowing a very detailed analysis of the exhaust solid.
A special filter studied by our group allows the operator to fill and empty the extractors only activating a system of valves, without touching the apparatus and avoiding dangerous contacts with hot surfaces.
Every extractor can work in series with the others or excluded from the system.
With this work, we want to approach as much as possible to an industrial context, making the scale-up of a process that currently takes place only at a laboratory scale.

Bibliography

[1] F. Cherubini, The biorefinery concept: Using biomass instead of oil for producing energy and chemicals, Energy Conversion and Management 51 (2010) 1412-1421.
[2] P. Mäki-Arvela, B. Holmbom, T. Salmi, D.Y. Murzin, Recent Progress in Synthesis of Fine and Specialty Chemicals from Wood and Other Biomass by Heterogeneous Catalytic Processes, Catalysis Reviews: Science and Engineering 49 (2007) 197 - 340.
[3] M. González, A. García, A. Toledano, R. Llano-Ponte, M.A. De Andrés, J. Labidi, Lignocellulosic feedstock biorefinery processes. Analysis and design, 2009, pp. 1107-1112.
[4] T. Salmi, Chemical Reaction Engineering of Biomass Conversion, 2013, pp. 195-260.
[5] J.J. Bozell, G.R. Petersen, Technology development for the production of biobased products from biorefinery carbohydrates-the US Department of Energy's "Top 10" revisited, Green Chemistry 12 (2010) 539-554.
[6] P. Mäki-Arvela, T. Salmi, B. Holmbom, S. Willför, D.Y. Murzin, Synthesis of sugars by hydrolysis of hemicelluloses- A review, Chemical Reviews 111 (2011) 5638-5666.
[7] H. Grenman, K. Eranen, J. Krogell, S. Willfor, T. Salmi, D.Y. Murzin, Kinetics of aqueous extraction of hemicelluloses from spruce in an intensified reactor system, Industrial and Engineering Chemistry Research 50 (2011) 3818-3828.
[8] D. Cantero, M.D Bermejo, M.J. Cocero, Kinetic analysis of cellulose depolymerization reactions in near critical water, The Journal of Supercritical Fluids 75 (2013) 48– 57.

Acknowledgements

The authors acknowledge the Spanish Economy and Competitiveness Ministry, Project FracBioFuel: ENE2012-33613 and the regional government (Junta de Castilla y León), Project Reference: VA330U13 for funding. MEng. Gianluca Gallina wish to acknowledge the Spanish Economy and Competitiveness Ministry for the scholarship/predoctoral contract.

Intensification of the Extraction Process of Ferulic Acid from Wheat Bran by means of Pressurized Aqueous Ethanol

M. Victoria Pazo Cepeda

High Pressure Processes Group, Department of Chemical Engineering and Environmental Technology, University of Valladolid, Valladolid, Spain

1. Introduction

Phenolic compounds are of considerable interest due to their antioxidant properties. These compounds possess an aromatic ring bearing one or more hydroxyl groups and their structures may range from that of a simple phenolic molecule to that of a complex high-molecular weight polymer. [1]

Among all the phenolic compounds, ferulic acid (FA) is widely used in food, pharmaceutical and cosmetic industries due to its beneficial physiological effects such as anti-oxidant, anti-microbial, anti-thrombosis and anti-cancer activities [2-5].

It is the most abundant hydroxycinnamic acid found in wheat grain, and is mainly located in the aleurone layer. This layer is obtained in the bran fraction after the milling process of the grain and, as wheat bran is an abundant agroindustrial coproduct but only 10% of it is used for human consumption [6], extraction of ferulic acid from wheat bran represent a great opportunity to add value to this subproduct. The main inconvenient is that the major part of the FA is in an insoluble bound form, esterified to the arabinoxylans (AX) and other cell wall structural components (≈92%) [7]. Hence, new processes are required to break these bonds in order to recover it in high quantities.

Several pre-treatments can be applied: thermic, enzymatic, alkaline or acid hydrolysis, steam explosion and pressurized solvents are examples of them [8]. Pressurized solvent assisted extraction is a technique that uses a solvent above its boiling point with the pressure necessary to maintain it as liquid, which can modify greatly the properties of the solvent. The effect of the high temperature contribute not only to improve the mass transfer but also to break the links that maintain FA in its insoluble bound form.

In this project, pressurized aqueous ethanol was used to extract FA from wheat bran. Different mixtures of ethanol-water, at different temperatures and time of extraction were tested with the aim of obtaining the combination of them that maximizes the amount of ferulic acid extracted from wheat bran samples.

2. Material and Methods

A Box-Behnken experimental design was performed by using three factors and three levels: percentage of ethanol in the solvent (20-50-80 %), temperature (130-145-160 ºC)

and time of extraction (20-40-60 min). It resulted in 15 experiences, included 3 repetitions of the central point.

Each extraction was performed in a stainless steel batch reactor (total volume 140mL), where 2.6 g of wheat bran were mixed with 130 mL of the selected solvent. The mixture was stirred at 800 rpm and heated; when the desired temperature was reached, the time began to run. After time was over, a sample was taken and kept at 4ºC until it was analyzed.

Quantification of FA was performed by HPLC. For this analysis, 15 mL of solution from the reactor were evaporated to dryness in a rotary vacuum evaporator, and then reconstituted in 10 mL of aqueous methanol (50%).

3. Experimental results

The obtained results range from 50 to 300 µg of ferulic acid per gram of dry matter. The main effect plot for ferulic acid is shown in Figure 1. There, it can be seen that ferulic acid decrease with a higher content of ethanol in the solvent, and increase when temperature or time of extraction increase. Temperature contribute to break the bonds between FA and AX, and as higher is the temperature or longer is the time of extraction this effect is intensificated. Also, pressure and temperature affect the solvents properties. According to bibliography, at ambient conditions FA presents its highest solubility when using a mixture with 80% of ethanol [9], however at the tested conditions the lower the content of ethanol, the higher the extraction yields. Therefore, a solvent without ethanol (pressurized hot water) will be tested. Also, as no maximum has been reached, it is recommended to test higher times of extraction and/or temperature in order to find it.

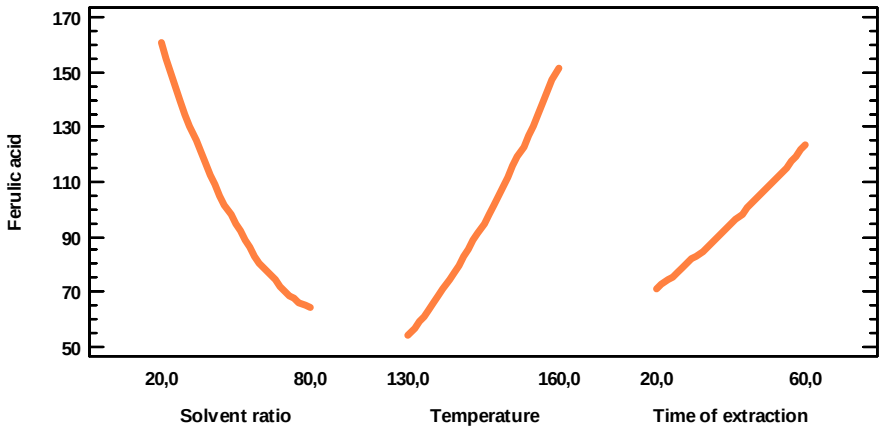

Figure 1. Main effect plot for ferulic acid extraction from wheat bran

Total ferulic acid and free ferulic acid in the raw material (obtained from alkaline hydrolysis) were 2523.86 µg/g and 11.86 µg/g, respectively (both in dry basis). The amount obtained with pressurized aqueous ethanol is much higher than the free fraction,

showing that is an effective way to brake these links and representing a more selective technique compared with the alkaline hydrolysis. However, there is still more ferulic acid available, so subsequent experiments are expected to produce bigger yields.

4. Conclusions

In this project, pressurized aqueous ethanol has been tested as solvent for the extraction of ferulic acid from wheat bran. It has been demonstrated to be a useful technique to break some of the bonds that link FA to the AX, as much more ferulic acid than the free one has been obtained. New experiments are going to be done in order to increase the amount of ferulic acid that can be extracted by the use of this technique.

5. References

1. Balasundram, N., K. Sundram, and S. Samman, *Phenolic compounds in plants and agri-industrial by-products: Antioxidant activity, occurrence, and potential uses.* Food Chemistry, 2006. **99**(1): p. 191-203.
2. Jacobs Jr, D.R., et al., *Whole-grain intake and cancer: An expanded review and meta-analysis.* Nutrition and cancer, 1998. **30**(2): p. 85-96.
3. Liu, S., et al., *Whole-grain consumption and risk of coronary heart disease: results from the Nurses' Health Study.* The American journal of clinical nutrition, 1999. **70**(3): p. 412-419.
4. McKeown, N.M., et al., *Whole-grain intake is favorably associated with metabolic risk factors for type 2 diabetes and cardiovascular disease in the Framingham Offspring Study.* The American journal of clinical nutrition, 2002. **76**(2): p. 390-398.
5. Liu, R.H., *Whole grain phytochemicals and health.* Journal of Cereal Science, 2007. **46**(3): p. 207-219.
6. Hossain, K., et al., *Interdependence of cultivar and environment on fiber composition in wheat bran.* Australian Journal of Crop Science, 2013. **7**(4): p. 525-531.
7. Brouns, F., et al., *Wheat aleurone: separation, composition, health aspects, and potential food use.* Critical reviews in food science and nutrition, 2012. **52**(6): p. 553-68.
8. Acosta-Estrada, B.A., J.A. Gutierrez-Uribe, and S.O. Serna-Saldivar, *Bound phenolics in foods, a review.* Food Chemistry, 2014. **152**: p. 46-55.
9. Buranov, A.U. and G. Mazza, *Extraction and purification of ferulic acid from flax shives, wheat and corn bran by alkaline hydrolysis and pressurised solvents.* Food Chemistry, 2009. **115**(4): p. 1542-1548.

AN ALTERNATIVE SOURCE OF POLYPHENOL-DERIVED COMPOUNDS: WINE LEES

Rut Romero Díez

High Pressure Processes Group, Department of Chemical Engineering and Environmental Technology, School of Engineering, University of Valladolid, Spain
Instituto de Biologia Experimental Tecnológica, Nutraceuticals and Delivery Lab, Portugal

rut.romero@itqb.unl.pt

Grapes are one of the most abundant cultivated crops over the world, around 60 million metric tons are produced annually [1]. Approximately, eighty percent of the worldwide is used in the winery production. One of the problems associated with this agronomic activity is the huge quantity of residues generated. These wastes are produced, mainly, during the wine fermentations and they constitute a serious problem due to the contamination of the environment. Chiefly, these residues consist on grape stalks, grape pomace and wine lees. The latter are produced during wine aging and maturation in the second fermentation [2]. In this fermentation anthocyanins undergo diverse reactions and transformations with organic compounds, phenolic acids or flavonoids yielding new anthocyanin-derived structures named pyranoanthocyanins [3]. The combination of these pyranoanthocyanins, the yeast responsible of the fermentation, other free phenolic compounds and metabolites constitute the *"wine lees".*

Figure 1: different types of residues produced during vinification process: grape stalks, grape pomace and wine lees.

This big amount of waterwastes constitute a serious problem due to the contamination of the environment and the outlays related to treat them are still very high. However, these residues are rich in phenolic compounds and high added value products can be obtain from them, such as natural pigments, natural antioxidants or health-promoting ingredients...

The aim of the herein project is the recovery of high valued products, such as those mentioned before, from different wine lees, in a background of a concept of a biorefinery and

bioeconomy developing new green processes and methodologies for their extraction, fractionation and purification (and increasing selectivity and yield).

The study of the process starts from the gathering of the wine less until the target compounds are separated and isolated. Once the wine lees are gathered, they should be separated from the liquid phase by centrifugation and two phases are obtain which will be treat separately. On one hand, the liquid phase is analyzed by different methods such as TPC (Total Polyphenol Content by Folin Ciocalteu method), FVC (Flavonoid Content), etc. Depending on the results obtained from these methods, a SAS process (Supercirtical Anti-Solvent) could be applied and/or a solid-liquid adsorption process with commercial resins could be carried on in order to separate the different compounds.

On the other hand, the solid phase will be pretreated to eliminate all the moiety and obtain a dried solid. This solid will pass through a matrix characterization with different solvents. Some analysis like TPC and FVC will be carried out to the different extracts. Also, an exhaustively study in the identification of the compounds present in each extract is being performed using HPLC-DAD-UV and HPLC-MS, in particular to identify the novel anthocyanins-derived compounds which are supposed to have a high antioxidant activity.

In the following figure a summary of the whole process can be seen.

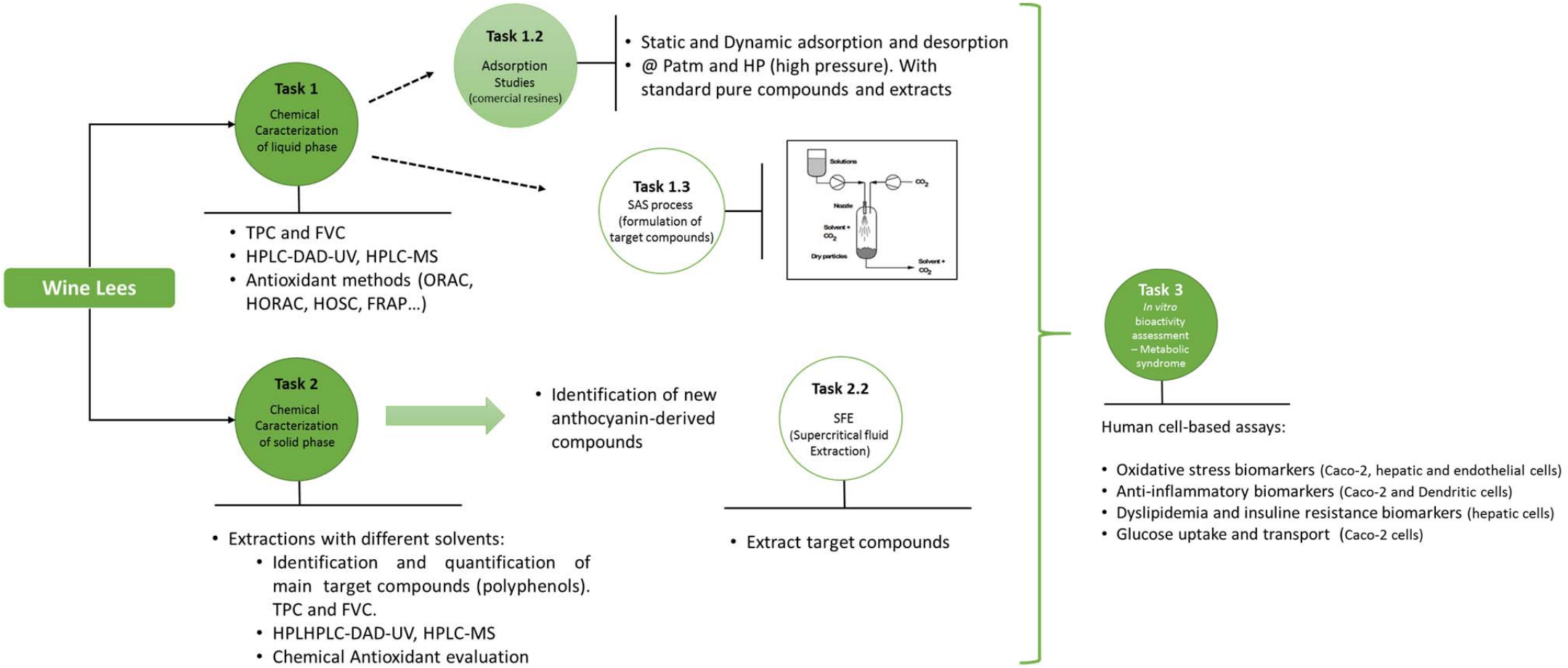

Figure 2: schematic representation of all the tasks of the whole project

BIBLIOGRAPHY

[1] A. Marquez, M. P. Serratosa, and J. Merida, “Pyranoanthocyanin derived pigments in wine: Structure and formation during winemaking,” Journal of Chemistry. 2013.

[2] N. Mateus, J. Oliveira, M. Haettich-Motta, and V. de Freitas, “New Family of Bluish Pyranoanthocyanins,” J. Biomed. Biotechnol., vol. 2004, pp. 299–305, 2004.

[3] N. Mateus, A. M. S. Silva, J. C. Rivas-Gonzalo, C. Santos-Buelga, and V. De Freitas, “A new class of blue anthocyanin-derived pigments isolated from red wines,” J. Agric. Food Chem., vol. 51, pp. 1919–1923, 2003

Supercritical-assisted hot melt extrusion: biopolymer foams elaboration and process modelling

Margot CHAUVET, Jacques FAGES, Martial SAUCEAU
RAPSODEE Research Centre, Ecole des Mines d'Albi, CNRS, F-81013 Albi, France

Polymeric foams are used in many fields because they have a low density and they present insulation properties. Depending on the cell morphology of the foam, the applications are varied. A close-cell morphology foam is generally use for the packaging, construction or heat insulation whereas an open-cell morphology foam is preferably use for the shock absorption, sound attenuation and tissue engineering (Gong & Ohshima 2015).

As the foams are used in many domains, nowadays there is great interest to replace the petroleum-based polymers by biopolymers in the aim of waste reduction and preservation of the petroleum resource. Indeed, the biopolymers are made from renewable resources and present comparable properties with the synthetic polymers. The poly(lactic acid) (PLA), a thermoplastic biopolyester obtained by fermentation of renewable resource like corn starch, is a promising polymer that can substitute traditional petroleum based plastics. The PLA can be amorphous or semi-crystalline, it shows good mechanical properties, tensile modulus higher than polypropylene (PP), polystyrene (PS) and high density polyethylene (HDPE). This polymer is also biodegradable, compostable and biocompatible (Lim et al. 2008).

Among the several technologies for polymer foam production, the extrusion assisted by supercritical carbon dioxide (sc-CO_2) is one of the most promising. Indeed, the main advantage of the use of sc-CO_2 is its high solubility in numerous polymers. In consequence, it acts as a plasticizer that will decrease the viscosity of the materials in the barrel of the extruder and also as a foaming agent with the return to atmospheric pressure at the die exit (Sauceau et al. 2011).

The aim of my PhD subject is the study of biopolymer foam production by the process of extrusion assisted by sc-CO_2. The biopolymer chosen for this work is the poly(lactic acid) because of the well-known good solubility of the CO_2 (Nofar & Park 2014). Furthermore, as the PLA is a biobased, biodegradable and biocompatible polymer, it could be use in many fields like the packaging or in the medical. For these multiple applications, it is thus essential to design foams with various and controlled properties. Moreover, the PLA usually exhibits a low crystallinity, which impacts directly its barrier properties and heat deflection temperature. The keys for controlling the properties of the foams are the formulation of the matrix and the processing parameters. It has already been shown the foaming with extrusion assisted by sc-CO_2 is a promising method to develop a high crystallinity, because of the plasticization effect of the pressurized CO_2 and the biaxial extension that occurs during pore (Mihai et al. 2009, Keshtkar et al. 2014). Moreover, to improve the functional properties of the PLA, we have chosen to add some additives to the PLA, like starch and/or mineral particles.

The foams are manufactured by a single-screw extruder of 30 mm screw diameter and a length to diameter ratio (L/D) of 37 (Rheoscam, SCAMEX) as shown in Fig. 1. The screw is divided into three sections. A restriction ring is located between each section to prevent backflow of CO_2. The polymer is introduced in the feed hopper.

Carbon dioxide is pumped from a cylinder by a syringe pump operating in constant volumetric flow rate mode. The CO_2 is introduced at the same pressure as the polymer in the extruder by an injector positioned at a length to diameter ratio of 20 from the feed hopper.

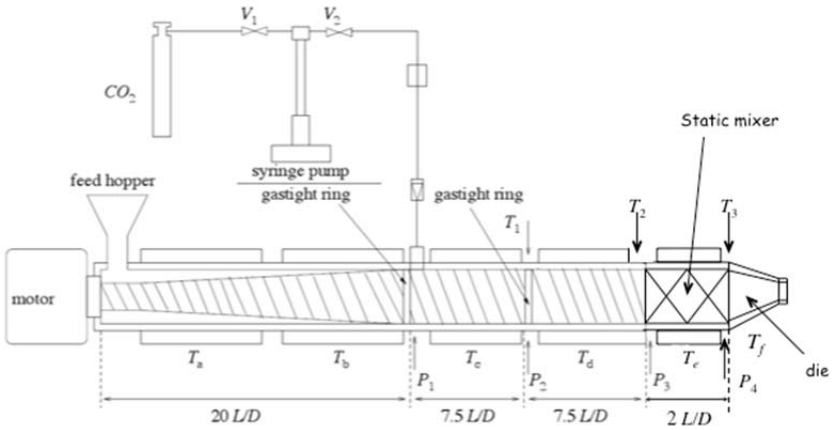

Fig. 1 : The experimental device used in this study (Rheoscam, SCAMEX)

The characterisations made on the foam are physical (measurement of the porosity and the density of the samples), thermal (measurement of the glass transition temperature, melt temperature and crystallisation temperature by DSC) and morphological (observation of the cell by SEM). It would be interesting to measure the barrier properties of our samples if the morphology is close-cell, whereas if our samples present an open-cell morphology, we could measure some mechanical properties like shock absorption.

The first part of this study is devoted to the foaming of raw PLA and the control of the morphology. The PLA used is the PLE001 grade from NaturePlast. For all the experimentation, the screw speed is fixed at 30 rpm and the temperature of the barrel between T_a and T_d is fixed at 160-180-180-160°C. The temperatures T_e and T_f range between 100 and 140°C. The volumetric flow of sc-CO_2 ranges between 2 and 4 mL/min. The Fig. 2 shows the porosity of our samples as a function of temperatures T_e and T_f. This figure shows that to get a high porosity foam (up to 95 %) it is necessary to decrease the temperature and, for that, to increase the sc-CO_2 ratio.

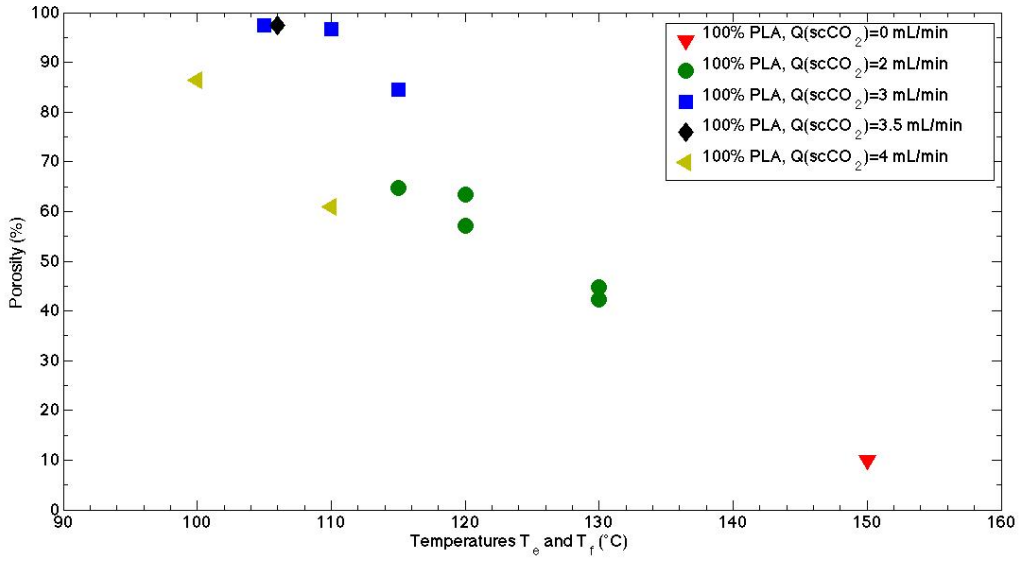

Fig. 2: The porosity in function of temperature T_e and T_f

Table 1 shows the temperatures T and enthalpies ΔH characteristics in the first heating in DSC. The subscripts g, cc and m are associated to glass transition, cold crystallisation and melting respectively. This table shows that the process of extrusion assisted by sc-CO_2 increases the crystallinity χ_c of the neat PLA. The high crystallinity of our sample is directly linked with the high porosity as shown in the Fig. 2.

Sample	T_g (°C)	T_{cc} (°C)	ΔH_{cc} (J/g)	T_{m1} (°C)	ΔH_{m1} (J/g)	T_{m2} (°C)	ΔH_{m2} (J/g)	χ_c (%)
Extruded PLA (150°C, 0 mL/min)	56	100	26.3	145	11.3	152	16.1	1.2
Foam of PLA (110°C, 3 mL/min)	59	78	11.5	150	29.4			19.2
Foam of PLA (105°C, 3 mL/min)	58	73	5.2	148	31.5			28.3

Table 1: The temperatures and enthalpies characteristics of PLA extruded samples during the first heating in DSC

The second part of this study concerns a blend of PLA with native starch. The starch used in this part will be a cornstarch from Roquette. The blend is made manually with 95% PLA and 5% starch. The processing conditions are the same as for the virgin polymer. We expect an increase of the crystallinity of the blends with the introduction of the native starch (Battegazzore et al. 2014).

It is reported in the literature that the PLA and the starch are two immiscible polymers (Martin & Avérous 2001). The gelatinization of the starch, by adding plasticizers like the glycerol, can enhance the interfacial adhesion between this two polymers (Ayana et al. 2014). The third part of this work focus on a blend made with PLA and a commercially thermo-plasticized starch (NPWS001, NaturePlast).

Bibliography

Ayana, B., Suin, S. & Khatua, B.B., 2014. Highly exfoliated eco-friendly thermoplastic starch (TPS)/poly (lactic acid)(PLA)/clay nanocomposites using unmodified nanoclay. *Carbohydrate polymers*, 110, pp.430–9.

Battegazzore, D., Alongi, J. & Frache, A., 2014. Poly(lactic acid)-Based Composites Containing Natural Fillers: Thermal, Mechanical and Barrier Properties. *Journal of Polymers and the Environment*, 22(1), pp.88–98.

Gong, P. & Ohshima, M., 2015. Open-Cell Foams of Polyethylene Terephthalate/Bisphenol A Polycarbonate Blend. *Polymer Engineering and Science*, 55, pp.375–385.

Keshtkar, M. et al., 2014. Extruded PLA/clay nanocomposite foams blown with supercritical CO2. *Polymer*, 55(16), pp.4077–4090.

Lim, L.-T., Auras, R. & Rubino, M., 2008. Processing technologies for poly(lactic acid). *Progress in Polymer Science*, 33, pp.820–852.

Martin, O. & Avérous, L., 2001. Poly(lactic acid): Plasticization and properties of biodegradable multiphase systems. *Polymer*, 42, pp.6209–6219.

Mihai, M., Huneault, M. a. & Favis, B.D., 2009. Crystallinity development in cellular poly(lactic acid) in the presence of supercritical carbon dioxide. *Journal of Applied Polymer Science*, 113(5), pp.2920–2932.

Nofar, M. & Park, C.B., 2014. Poly (lactic acid) foaming. *Progress in Polymer Science*, 39(10), pp.1721–1741.

Sauceau, M. et al., 2011. New challenges in polymer foaming: A review of extrusion processes assisted by supercritical carbon dioxide. *Progress in Polymer Science*, 36(6), pp.749–766.

Registered Lecturers

Prof. Zeljko Knez	University of Maribor, Slovenia zeljko.knez@uni-mb.si
Prof. Thomas Gamse	Graz University of Technology, Austria thomas.gamse@tugraz.at
Dr. Eduard Lack	Natex Prozesstechnologie, Austria office@natex.at
Dr. Helena Sovova	Academy of Sciences of the Czech Republic, Czech Republic, sovova@icpf.cas.cz
Dr. Dominik Lanzinger	BASF SE GME/D- Polymer Process Development, Germany, dominik.lanzinger@basf.com,
Kerstin Gerling	BASF SE GME/D- Polymer Process Development, Germany, kerstin.gerling@basf.com
Prof. Marcus Petermann	Ruhr University Bochum, Germany petermann@fvt.ruhr-uni-bochum.de
Prof. Markus Busch	Technical University Darmstadt, Germany busch@chemie.tu-darmstadt.de
Prof. Eberhard Schlücker	University Erlangen Nürnberg, Germany sl@ipat.uni-erlangen.de
Dr. Carsten Zetzl	Technical University Hamburg Harburg, Germany zetzl@tu-harburg.de
Prof. Maria Jose Cocero	University of Valladolid, Spain mjcocero@iq.uva.es
Prof. Jacques Fages	Ecole des Mines d'Albi, France Jacques.Fages@enstimac.fr
Prof. Edit Szekely	Budapest University of Technology and Economics, Hungary, sz-edit@mail.bme.hu
Prof. Ireneo Kikic	University of Trieste, Italy ireneo.kikic@gmail.com

Prof. Alberto Bertucco	University of Padua, Italy alberto.bertucco@unipd.it
Prof. Theo de Loos	Technical University Delft, The Netherlands T.W.deLoos@tudelft.nl
Prof. Ludo Kleintjens	DSM Company / Ruhr University Bochum, The Netherlands, ludo.kleintjens@hetnet.nl
Dr. Rita Duarte	University of Minho, Portugal aduarte@dep.uminho.pt
Prof. Manuel Nunes da Ponte	New University of Lisbon, Portugal mnponte@fct.unl.pt
Prof. Irena Zizovik	University of Belgrade, Serbia zizovic@tmf.bg.ac.rs
Prof. Can Erkey	KOC University Istanbul, Turkey cerkey@ku.edu.tr
Prof. Carl Schaschke	Abertay University, United Kingdom c.schaschke@abertay ac.uk

Registered Participants

Neven Tutnjević	University of Maribor,	Slovenia
Gregor Kravanja	University of Maribor,	Slovenia
Jaroslav Lang	Academy of Sciences of the Czech Republic,	Czech Republic
Dominik Lanzinger	BASF SE Polymer Process Development	Germany
Kerstin Gerling	BASF SE Polymer Process Development	Germany
Judith Kremer	Ruhr University Bochum	Germany
Rebecca Scholz	Ruhr University Bochum	Germany
Ricarda Kendler	Ruhr University Bochum	Germany
Olga Melchaeva	Ruhr University Bochum	Germany
Margarita Balyschewa	Technical University Darmstadt	Germany
Kristina Zentel	Technical University Darmstadt	Germany
Sascha Griebenow	Technical University Darmstadt	Germany
Kevin Vogel	Technical University Darmstadt	Germany
Anna Carina Kimmel	University Erlangen Nürnberg	Germany
Manuel Zürcher	University Erlangen Nürnberg	Germany
Hannah Singer	Technical University Hamburg Harburg	Germany
Imke Meissner	Technical University Hamburg Harburg	Germany
Fynn Mißfeldt	Technical University Hamburg Harburg	Germany
Daniel Deodato Lopes	University of Valladolid	Spain
Gianluca Gallina	University of Valladolid	Spain
María Victoria Pazo Cepeda	University of Valladolid	Spain
Rut Romero Díez	University of Valladolid	Spain
Margot Chauvet	Ecole des Mines d'Albi	France